EVOLUTIONARY BIOLOGY

# Two horizontally acquired bacterial genes steer the exceptionally efficient and flexible nitrogenous waste cycling in whiteflies

**Zezhong Yang[1,2]†, Zhaojiang Guo[1]†, Cheng Gong[1]†, Jixing Xia[1]†, Yuan Hu[1], Jie Zhong[1], Xin Yang[1], Wen Xie[1], Shaoli Wang[1], Qingjun Wu[1], Wenfeng Ye[3], Baiming Liu[2], Xuguo Zhou[4], Ted C. J. Turlings[3]*, Youjun Zhang[1]***



**Nitrogen is an essential element for all life on earth. Nitrogen metabolism, including excretion, is essential for growth, development, and survival of plants and animals alike. Several nitrogen metabolic processes have been described, but the underlying molecular mechanisms are unclear. Here, we reveal a unique process of nitrogen metabolism in the whitefly *Bemisia tabaci*, a global pest. We show that it has acquired two bacterial uricolytic enzyme genes, *B. tabaci urea carboxylase* (*BtUCA*) and *B. tabaci allophanate hydrolase* (*BtAtzF*), through horizontal gene transfer. These genes operate in conjunction to not only coordinate an efficient way of metabolizing nitrogenous waste but also control *B. tabaci*'s exceptionally flexible nitrogen recycling capacity. Its efficient nitrogen processing explains how this important pest can feed on a vast spectrum of plants. This finding provides insight into how the hijacking of microbial genes has allowed whiteflies to develop a highly economic and stable nitrogen metabolism network and offers clues for pest management strategies.**

## INTRODUCTION

Nitrogen is an essential building block for all living organisms. Most plants absorb and assimilate inorganic nitrogen in their roots (*1*, *2*). Animals, and even some plants, acquire organic nitrogen, mainly amino acids, from their organic diet (*1*, *3*, *4*). For them, the acquired nitrogen is like a double-edged sword. On one side, it is used to synthesize proteins, nucleotides, and other important nitrogen-containing compounds that are essential for development, reproduction, and interactions (*2*, *3*, *5*, *6*). But on the other side, its nitrogen metabolism results in toxic nitrogen-containing intermediates. These intermediates can damage proteins, DNA, and cells (*7*, *8*), and in animals, this can cause inflammations, gout, and even cancers (*6*, *9*–*11*).

To mitigate the harm resulting from nitrogen metabolism, animals convert acquired nitrogen products into waste that can be excreted. Excretion of nitrogenous waste products can be as important as proper nitrogen metabolism for the survival and development. Nearly all terrestrial animals export uric acid or urate salt as final waste products (*12*). However, several exceptions exist, with insects contributing largely to those exceptions. For instance, cockroaches export ammonia as their ultimate nitrogenous waste (*13*). Other well-known exceptions are sap-feeding insects. These insects, such as whiteflies, aphids, and planthoppers, excrete free amino acids rather than uric acid (*14*–*16*). In the case of cockroaches, the final step toward nitrogenous waste biosynthesis involves uricolytic enzymes provided by their obligate symbionts (*17*). For sap-feeding insects, although their unique waste products are well known (*14*, *15*), the underlying molecular and biosynthetic mechanisms are still unclear.

Besides being excreted, nitrogenous waste can also be stored by certain animals, allowing them to salvage urea to synthesize essential amino acids (*18*–*20*). Certain insects, such as cockroaches (*21*), termites (*22*), and planthoppers (*23*), have thus evolved highly efficient nitrogen recycling mechanisms that allow them to convert nitrogenous waste into nutrients when the insects are faced with insufficient external nitrogen availability (*17*). Mutualistic bacteria appear to be key factors in this nitrogen recycling (*21*–*23*). With genes encoding uricolytic enzymes, the mutualistic bacteria convert urea to ammonia, which can then be used to synthesize amino acids. Hence, the mutualists provide their hosts with the ability to cope with unfavorable nutritional conditions. In all reported cases, the animals fully rely on mutualistic relationships with endosymbiotic bacteria or gut bacteria (*20*, *23*). There appear to be no reports of animals able to independently salvage or recycle nitrogen.

The whitefly, *Bemisia tabaci* (Gennadius), a well-known sap-feeding insect, is a devastating worldwide pest that comprises at least 30 cryptic species, among which the Mediterranean (MED) and Middle East-Asia Minor 1 (MEAM1) are the most widespread and damaging (*24*, *25*). *B. tabaci* not only causes feeding damage but also transmits plant viruses and provokes fungal diseases, thereby seriously hampering agricultural production and causing billions in economic losses every year (*26*, *27*). *B. tabaci* is highly polyphagous and shows tremendous host plant adaptability, which explains its extreme global spread (*28*, *29*). Plants vary greatly in nitrogen contents (*30*), which poses a considerable nutritional challenge to herbivorous insects (*31*, *32*). Unraveling how *B. tabaci* is able to ensure an economic and stable nitrogen metabolism could aid in understanding how it survives on its many different host plants and be of great importance for crop protection. As it is increasingly evident that much of the whitefly's metabolism is under control of horizontally acquired genes (*29*, *33*, *34*), we hypothesized that such genes may also serve in its nitrogen metabolism.

[1]State Key Laboratory of Vegetable Biobreeding, Department of Plant Protection, Institute of Vegetables and Flowers, Chinese Academy of Agricultural Sciences, Beijing 100081, China. [2]Institute of Plant Protection, Tianjin Academy of Agricultural Sciences, Tianjin 300381, China. [3]Laboratory of Fundamental and Applied Research in Chemical Ecology, Institute of Biology, University of Neuchâtel, CH-2000 Neuchâtel, Switzerland. [4]Department of Entomology, University of Kentucky, Lexington, KY 40546-0091, USA.
*Corresponding author. Email: ted.turlings@unine.ch (T.C.J.T.); zhangyoujun@caas.cn (Y.Z.)
†These authors contributed equally to this work.

Here, we reveal that *B. tabaci urea carboxylase* (*BtUCA*) and *B. tabaci allophanate hydrolase* (*BtAtzF*), two bacteria-derived genes, are integrated into the *B. tabaci* genome and that these genes serve as key switches in the nitrogen metabolism, allowing for nitrogenous waste biosynthesis, as well as nitrogen recycling. These horizontally acquired traits explain, at least in part, *B. tabaci*'s incredible host plant adaptability. They also provide clues as to why fertilizer applications often lead to whitefly outbreaks (*35*–*38*). These findings can be the basis for the development of new strategies to control this exceedingly important pest.

## RESULTS

### Construction of nitrogenous waste biosynthesis pathway in *B. tabaci*

We used a multi-omics approach to construct the complete nitrogenous waste biosynthesis pathway in *B. tabaci* MED (Fig. 1A). In the metabolome analysis, a total number of 1415 peaks were detected and, of these, 828 peaks representing 377 compounds were identified (Fig. 1B and table S1). These included uric acid and several predicted intermediates of uricolytic pathways including xanthine, allantoate, and urea (Fig. 1B), which suggests that *B. tabaci* MED is able to degrade uric acid. Further, an isotope labeling experiment was conducted to investigated the uricolytic pathway of *B. tabaci* MED. After being fed with $^{15}N$-labeled glutamic acid, $^{15}N_2$-labeled urea, $^{15}N$-labeled aspartic acid, $^{15}N_2$-labeled asparagine, and $^{15}N_2$-labeled glutamine were all detected in *B. tabaci* MED adults' bodies (table S2). In addition, $^{15}N$-labeled aspartic acid, $^{15}N_2$-labeled asparagine, and $^{15}N_2$-labeled glutamine were detected in the honeydew of *B. tabaci* MED (table S2).

We also mined the uricolytic pathways of *B. tabaci* MED and its symbionts. The results reveal that genes specifically encoded by *B. tabaci* MED largely control its uricolytic pathway, whereas none of the genes from its primary symbiont, *Candidatus* Portiera aleyrodidarum, or from its secondary symbionts, *Rickettsia* sp., *Candidatus* Hamiltonella defense, and *Cardinium* endosymbiont, were involved in uric acid degradation (Fig. 1C, fig. S1, and table S3). Although *allantoinase* (*hpxB*), *allantoinase* (*allB*), and *allantoicase* (*ALLC*) are absent in the genome of *B. tabaci* (Fig. 1C), typical products of *hpxB*, *allB*, and *ALLC* were found in the metabolome (Fig. 1B), indicating that several genes in *B. tabaci* MED have the same function as *hpxB*, *allB*, and *ALLC*. We propose that that these as yet unidentified genes are results of evolutionary innovation and that the limited current knowledge on uricolytic pathways in hemipteran insects prevents us from detecting them.

Meta-transcriptome sequencing was further used to ensure that gut bacteria did not contribute to the biosynthesis of nitrogenous waste in their host. Although the constitution and function of gut bacteria varied considerably among different geographical strains of *B. tabaci* MED and on different host plants (Fig. 1D and fig. S2), in no case did they harbor genes to construct a complete uricolytic pathway (Fig. 1E). On the basis of these findings, we hypothesized that the entire chain of nitrogenous waste biosynthesis in *B. tabaci* MED is controlled by the insect itself and is independent of any symbiotic organisms.

### Evidence for the horizontal transfer of *BtUCA* and *BtAtzF* from bacteria to *B. tabaci*

While constructing the nitrogenous waste biosynthesis pathway of *B. tabaci* MED, we identified and cloned *BtUCA* and *BtAtzF*, two common bacterial genes (fig. S3, A and D). The amino acid sequences of both *BtUCA* and *BtAtzF* were highly similar among the *B. tabaci* cryptic species (fig. S4, A and B), but blasting against GenBank database revealed that, except for homologs of *B. tabaci* MEAM1 (for *BtUCA*, XP_018917734.1 and for *BtAtzF*, XP_018903453.1), their next closest homologs were all bacterial proteins. Subsequent phylogenetic analyses showed that *BtUCA* or *BtAtzF* clustered with homologs of γ-bacteria (Fig. 2, C and F, and figs. S5 and S6). Genomic analyses were performed to confirm that *BtUCA* and *BtAtzF* were inserted into the genome of *B. tabaci* MED, and the results showed that both genes were surrounded by insect genes. The *BtUCA* genomic region located at scaffold 7 and the *BtAtzF* genomic region located at scaffold 4 were accurately assembled (Fig. 2, A and D). Genomic regions of both genes and their surrounding genes of *B. tabaci* MED shared highly conserved synteny with *B. tabaci* MEAM1 (Fig. 2, B and E). Furthermore, polymerase chain reaction (PCR) amplification of those genomic regions confirmed the assembly accuracy and ensured that both *BtUCA* and *BtAtzF* are integrated into the *B. tabaci* MED genome (Fig. 2, B and E, and fig. S7). Moreover, no homologs of either *BtUCA* or *BtAtzF* were identified in *Trialeurodes vaporariorum*, a sister taxon to *B. tabaci* MED and MEAM1. *B. tabaci* MED, *B. tabaci* MEAM1, *B. tabaci* Sub-Saharan Africa 1 (*B. tabaci* SSA1), *B. tabaci* Zhejiang1 (*B. tabaci* ZJ1), and *B. tabaci* New World (*B. tabaci* NW) belong to different genetic groups, across nearly all of the subgroups of *B. tabaci* cryptic species (*25*). It is therefore very likely that the two genes are present in the genome of all *Bemisia* species. We may presume that *Bemisia* acquired these genes between 86 and 35 million years ago when *Bemisia* had separated from *Trialeurodes* but had not yet divided into cryptic species (*39*).

### The spatiotemporal expression profiles of *BtUCA* and *BtAtzF*

Next, the spatiotemporal expression patterns of *BtUCA* and *BtAtzF* were determined by real-time quantitative PCR (qPCR). Results showed that both *BtUCA* and *BtAtzF* were expressed across all the developmental stages of *B. tabaci* MED (egg, first-second-, third-, fourth-instar nymphs, adults) and in all parts of *B. tabaci* adult bodies (head, thorax, abdomen, and wing). The transcript levels of both genes were significantly higher in the eggs than in the nymphs (fig. S3, B and E). Of all body parts, both genes were the most highly expressed in the head of *B. tabaci* adults (fig. S3, C and F). As the *B. tabaci* does not feed in the egg, the results are further proof that the measured gene expressions were not the result of bacterial contaminants in the food. *BtUCA* and *BtAtzF* showed remarkably similar patterns in their spatiotemporal expression profiles, suggesting that the genes act simultaneously in a common metabolism network.

### Enzymatic activities of BtUCA and BtAtzF proteins mediating urea degradation

To confirm that *BtUCA* and *BtAtzF* show the same functionality as in their donors, they were heterogeneously expressed in *Escherichia coli* in vitro and their recombinant proteins were purified (Fig. 3, A and B). Biochemical assays showed that the purified recombinant BtUCA protein displayed adenosine triphosphate (ATP)–dependent carboxylase activity toward urea ($V_{max}$ = 39.54 μmol $mg^{-1}$ $min^{-1}$), and the purified recombinant BtAtzF exhibited ammonia-generating activity toward allophanate ($V_{max}$ = 81.21 μmol $mg^{-1}$ $min^{-1}$) (Fig. 3, A and B). Similar to previous reports (*40*, *41*), our results suggested that *BtUCA* and *BtAtzF* retained their ancestral functions in urea degradation for *B. tabaci*.

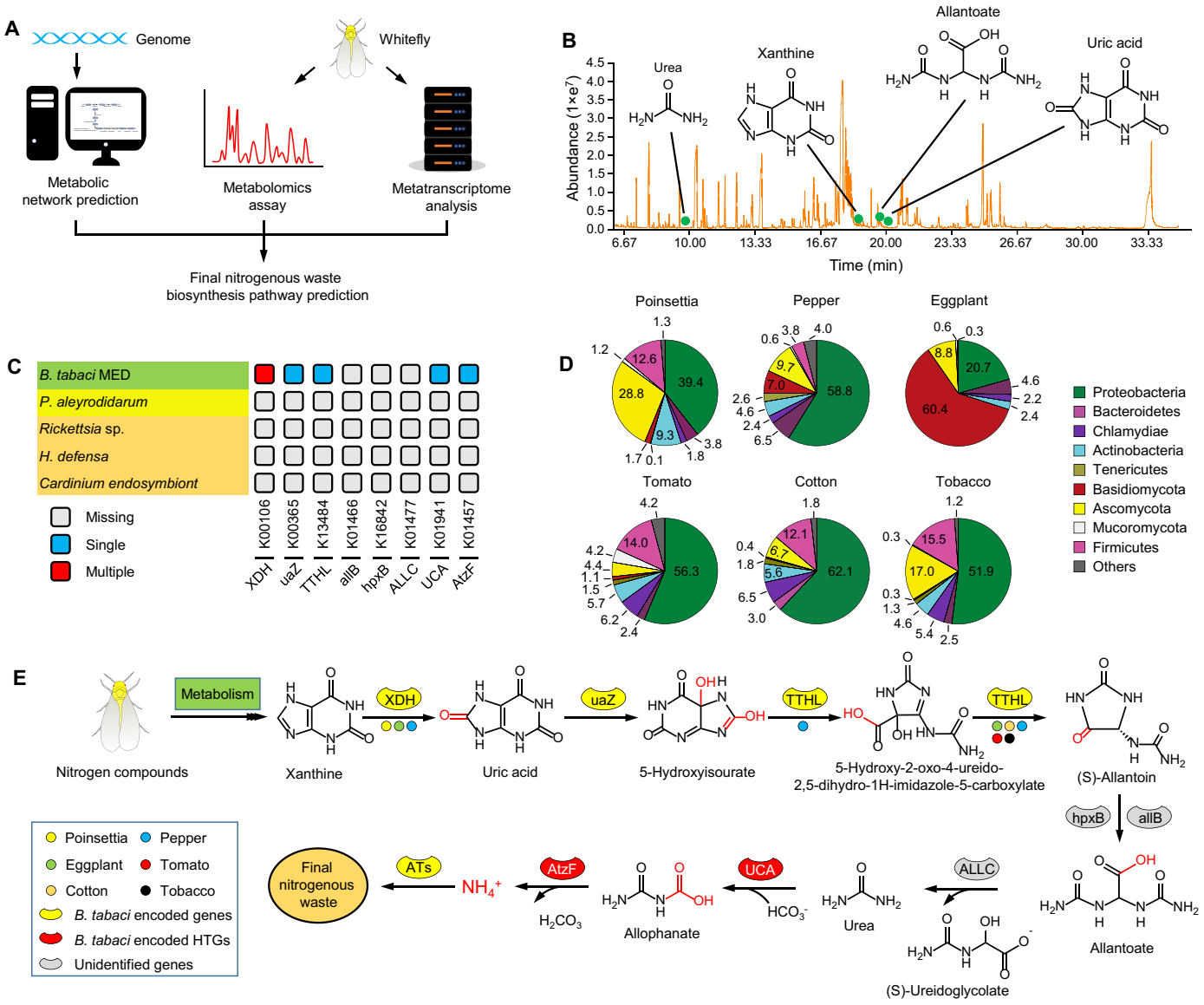


**Fig. 1. Characterization of the entire nitrogenous waste biosynthesis pathway of *B. tabaci*.** (**A**) The procedure for characterizing nitrogenous waste biosynthesis pathway of *B. tabaci*, which involved a multi-omics analysis process, that included a combination of genetic capacity, metabolome, and meta-transcriptome analyses. (**B**) Total ion chromatogram from a mass spectrometry–based metabolome analysis. (**C**) Genetic capacity analysis of genes related to nitrogenous waste biosynthesis in *B. tabaci* and its symbionts. *P. aleyrodidarum*, the primary symbiont of *B. tabaci*, is short for *Candidatus* Portiera aleyrodidarum and is indicated with a yellow background. *Rickettsia* sp., *H. defense*, and *Cardinium endosymbiont* are secondary symbionts of *B. tabaci* and are indicated with an orange background. *Rickettsia* sp. was identified as *Rickettsia* sp. strain MED. *H. defense* was identified as *Candidatus* Hamiltonella defense strain MED. *Cardinium endosymbiont* was identified as *Cardinium endosymbiont* strain MED. Gene symbols and KEGG Orthology (KO) numbers were obtained from KEGG (https://www.kegg.jp/kegg). (**D**) Classification of gut bacteria of *B. tabaci* MED based on meta-transcriptome analyses. (**E**) Constructed nitrogenous waste biosynthesis pathway of *B. tabaci*. Black arrows indicate reactions supported by genome annotation data or metabolome analysis. The nitrogenous waste biosynthesis–related genes identified in the gut bacteria of *B. tabaci* are shown as circles with different colors. Substrate structure changes in each reaction were labeled with red.

## Roles of *BtUCA* and *BtAtzF* on commanding a unique nitrogenous waste biosynthesis pathway

To further verify that *BtUCA* and *BtAtzF* participate in nitrogenous waste biosynthesis as predicted (Fig. 1E), two RNA interference (RNAi) approaches were applied. In the first approach, RNAi was achieved by feeding whiteflies an artificial diet spiked with double-stranded RNA (dsRNA) (Fig. 3C); *B. tabaci* MED adults were fed a diet containing gene-specific dsRNA that targeted *BtUCA* or *BtAtzF* individually, or both genes at the same time. qPCR analyses showed that the transcript levels of *BtUCA* and *BtAtzF* were significantly decreased upon silencing (Fig. 3, D and E). Moreover, silencing *BtUCA* and *BtAtzF* and cosilencing both genes significantly raised the urea content in *B. tabaci* (Fig. 3F) and reduced the amino acid content in whitefly honeydew (Fig. 3G). As urea was predicted to convert to free amino acids and excreted in honeydew, the results strongly indicate that *BtUCA* or *BtAtzF* participates in nitrogenous waste biosynthesis in *B. tabaci*.

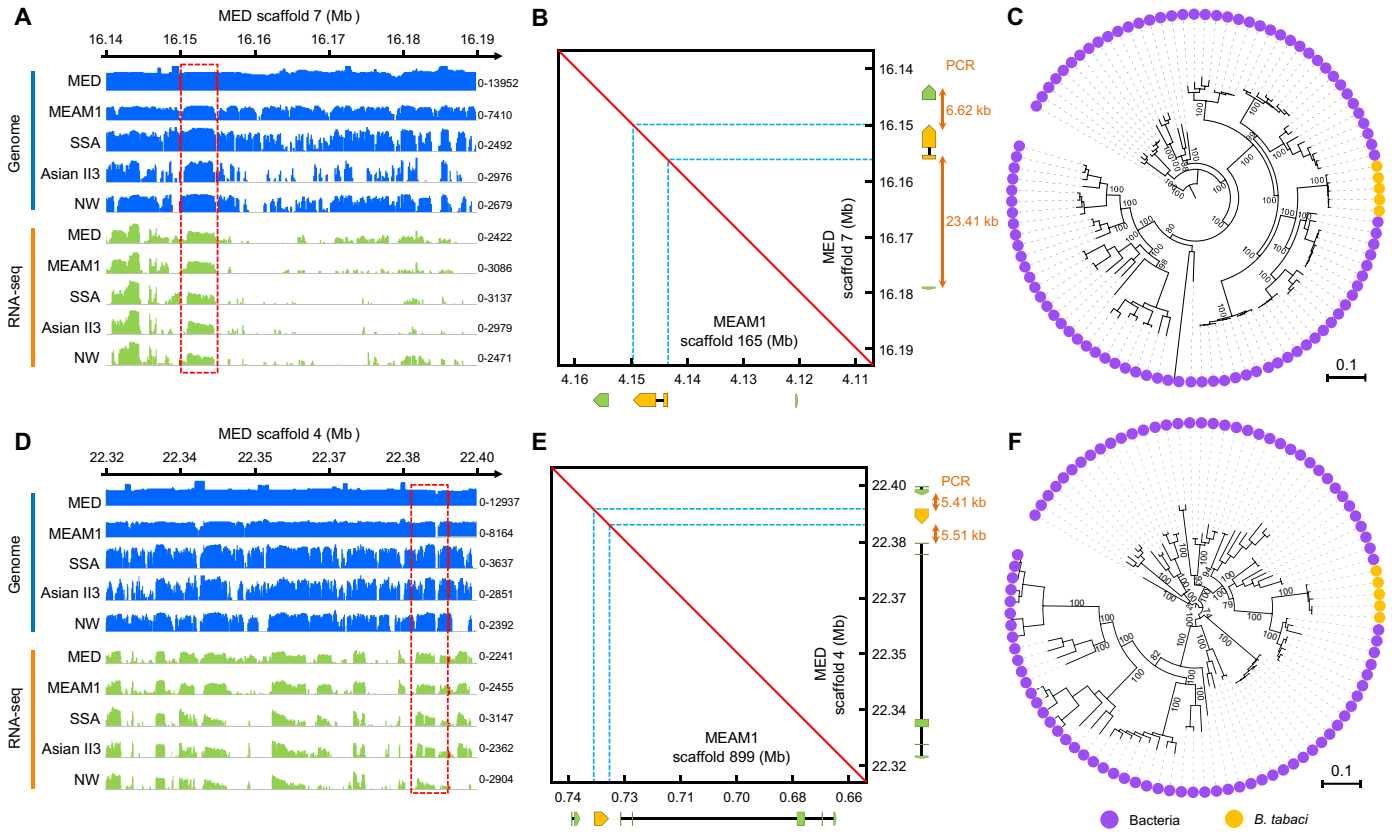


**Fig. 2. Evidence for the horizontal transfer of *BtUCA* and *BtAtzF* to *B. tabaci*.** (**A** and **D**) Genomic locations of *BtUCA* (A) and *BtAtzF* (D) in *B. tabaci* MED. The Illumina DNA-read coverage plots resulting from genomic sequencing of different *B. tabaci* cryptic species and Illumina RNA sequencing (RNA-seq) read coverage plots from adults of diverse *B. tabaci* cryptic species are shown. The sequencing depths are denoted by the numbers to the right of each coverage plot. (**B** and **E**) Genome synteny of the *BtUCA* (B) and *BtAtzF* (E) gene and their respective two surrounding genes in *B. tabaci* MED and *B. tabaci* MEAM1. The red diagonal line presents similarity of two genome regions above 95%. Genomic fragments cloned by PCR are indicated in orange. (**C** and **F**) Bayesian-based phylogenetic analysis of *BtUCA* (C) and *BtAtzF* (F) based on the optimized protein substitution matrixes. For both phylogenetic trees, β-proteobacteria proteins were used as outgroup for rooting the tree. The scale bar represents 0.1 amino acid substitutions per site. Only bootstrap values at phylogenetically important nodes are shown. *BtUCA* (C) and *BtAtzF* (F) are indicated with yellow circles. Bacterial proteins are indicated with purple circles.

In the second approach, virus-induced gene silencing (VIGS) experiments with tobacco plants were performed to further test the roles of *BtUCA* and *BtAtzF* in nitrogenous waste biosynthesis (Fig. 3H). Results from qPCR analyses showed that *BtUCA* and *BtAtzF* were significantly suppressed upon silencing (Fig. 3, I and K, and fig. S8, A and B). Knocking down either *BtUCA*, *BtAtzF*, or both genes at once significantly increased the urea content in *B. tabaci* (Fig. 3J and fig. S8C) and decreased the accumulation of amino acids in honeydew (Fig. 3L and fig. S8D). Hence, the results of the VIGS experiment were very similar to the results of the silencing via feeding capsules, and both RNAi approaches strongly suggested that *BtUCA* and *BtAtzF* play roles in nitrogenous waste biosynthesis.

## Nitrogenous waste biosynthesis under high-nitrogen stress in *B. tabaci*

After confirming the unique way in which *B. tabaci* synthesizes nitrogenous waste, we tested the possible involvement of the bacteria-derived genes in how *B. tabaci* manages high-nitrogen stress. In the first series of experiments, *B. tabaci* adults were fed artificial diets with different nitrogen contents (Fig. 4A). Higher levels of nitrogen in an artificial diet resulted in increased expression levels of both genes as well as higher amino acid levels excreted in honeydew (Fig. 4, B, D, and E). The involvement that the two bacteria-derived genes help *B. tabaci* overcome high-nitrogen stress was further investigated via isotope labeling approaches (fig. S10A). Feeding *B. tabaci* an artificial diet spiked with $^{15}$N-labeled glutamic acid caused increased levels of $^{15}N_2$-labeled asparagine (fig. S10B) and $^{15}N_2$-labeled glutamine (fig. S10D) in their honeydew as well as high expression levels of both *BtUCA* and *BtAtzF* (fig. S10, C and E). In the second series of experiments, we obtained similar results when *B. tabaci* were fed plants with different nitrogen contents, which was manipulated using different fertilization regimes (Fig. 4G). Again, the expression levels of *BtUCA* and *BtAtzF* and the content of amino acids in honeydew were significantly increased when the nitrogen contents in their host plant were raised (Fig. 4, H, J, and K). These results imply that *B. tabaci* uses the horizontally acquired genes to synthesize more nitrogenous waste when they are faced with high-nitrogen stress.

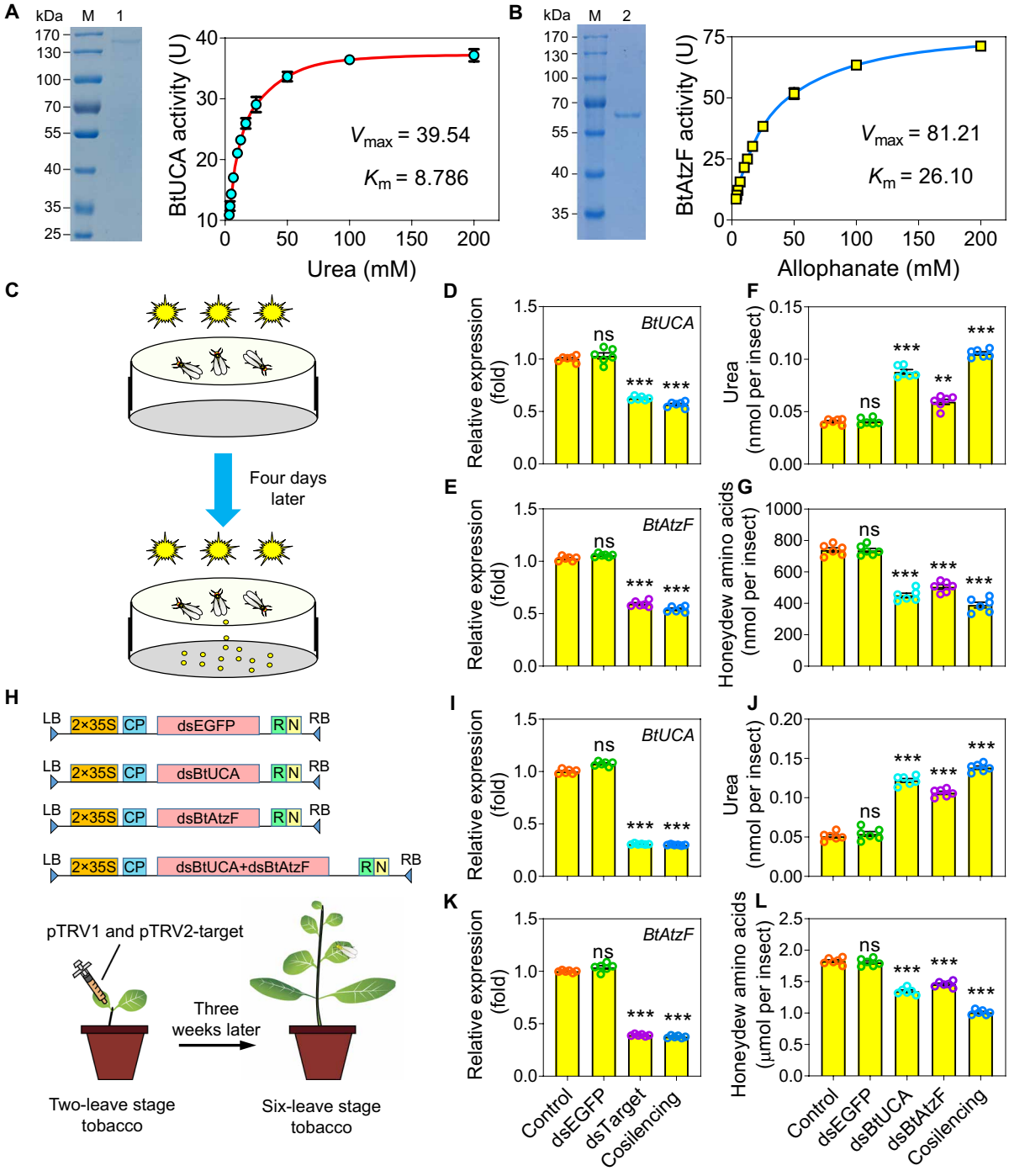


**Fig. 3. Roles of *BtUCA* and *BtAtzF* in nitrogenous waste biosynthesis of *B. tabaci*.** (**A** and **B**) Functional verification of *BtUCA* (A) and *BtAtzF* (B) by heterologous expression and protein purification. The enzymatic activities of recombinant BtUCA and BtAtzF proteins were measured. Standard Michaelis-Menten kinetics was calculated. M, protein marker; lane 1, recombinant BtUCA protein (A); lane 2, recombinant BtAtzF protein (B). (**C**) Schematic representation of the experimental design that investigated the roles of *BtUCA* and *BtAtzF* in nitrogenous waste biosynthesis using a dsRNA-feeding approach. To investigate the roles of *BtUCA* and *BtAtzF* in the nitrogenous waste biosynthesis of *B. tabaci*, gene-specific dsRNA (100 μg) was mixed into an artificial diet and the mixture was fed to insects for 4 days. (**D** and **E**) The transcript levels of *BtUCA* (D) and *BtAtzF* (E) at 96 hours post-RNAi as determined by qPCR. (**F**) Urea content of *B. tabaci* post-RNAi after 96 hours. (**G**) Honeydew amino acid content of *B. tabaci* post-RNAi after 96 hours. (**H**) Schematic representation of the experimental design that investigated the roles of *BtUCA* and *BtAtzF* on nitrogenous waste biosynthesis using VIGS plants. The construction of TRV-based VIGS vectors and procedure for persistent gene silencing of *B. tabaci* using TRV-infected plants. (**I** and **K**) Transcript levels of *BtUCA* (I) and *BtAtzF* (K) at 9 days post-RNAi as determined by qPCR. (**J**) Urea content of *B. tabaci* post-RNAi after 9 days. (**L**) Honeydew amino acid content of *B. tabaci* post-RNAi after 9 days. Data are presented as mean values ± SEM (B); $n = 3$ (A and B), $n = 6$ (C to K) biologically independent samples; $^*P < 0.05$, $^{**}P < 0.01$, $^{***}P < 0.001$; ns, not significant; one-way ANOVA with Dunnett's test was used for comparison.

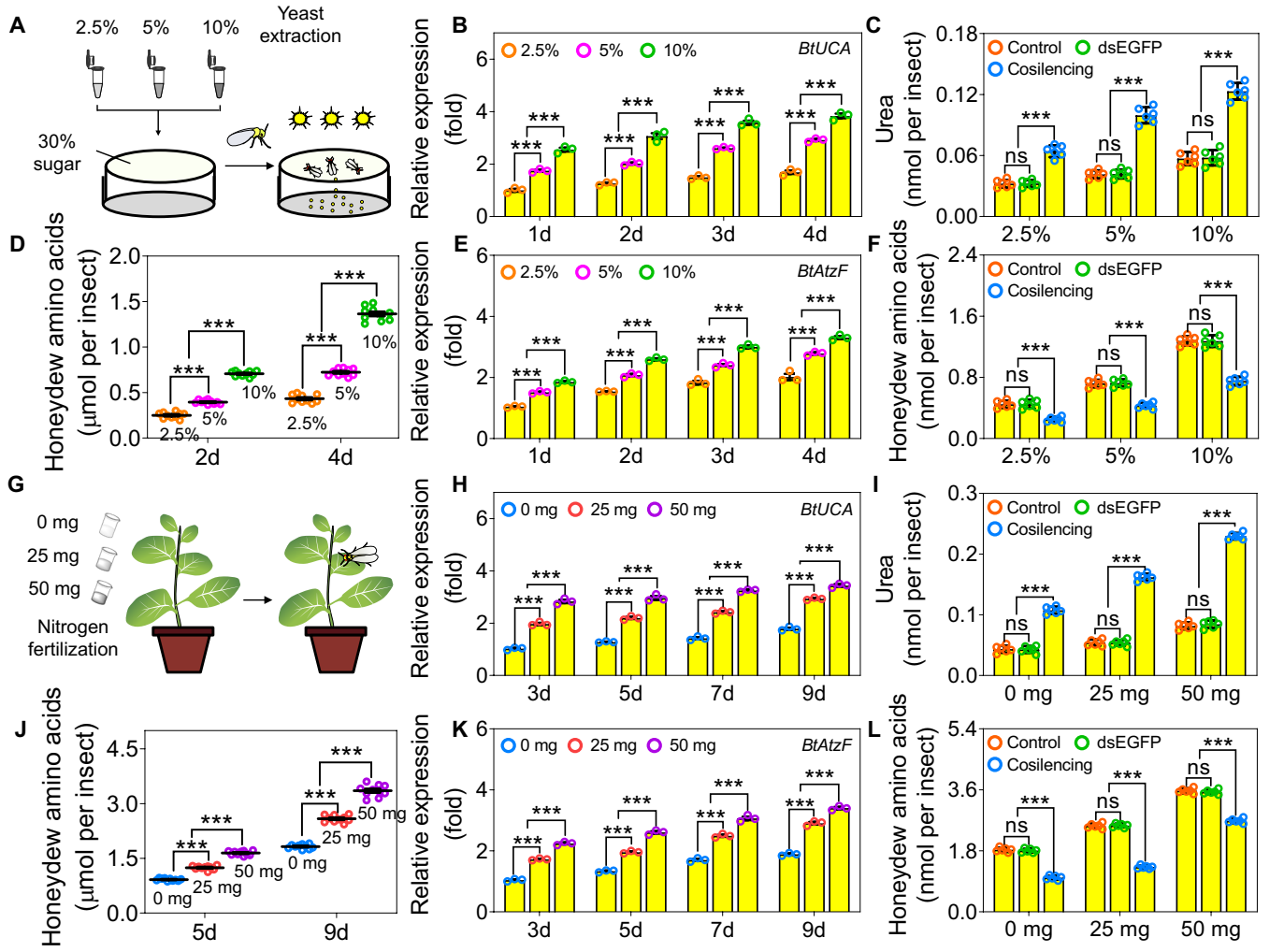


**Fig. 4. The role of *BtUCA* and *BtAtzF* in mitigating high-nitrogen stress in *B. tabaci*.** (**A**) Schematic representation of the high-nitrogen stress assays in which *B. tabaci* adults were fed an artificial diet with different nitrogen contents. Whiteflies were initially reared on tobacco plants (without nitrogen supplement). Then, the newly emerged whiteflies were collected and fed an artificial diet containing three different nitrogen levels (2.5%, 5%, or 10% yeast extract). (**B**, **D**, and **E**) The transcript levels of *BtUCA* (B) and *BtAtzF* (E) and the honeydew amino acid levels (D) after *B. tabaci* had fed a diet with different nitrogen contents for 4 days. (**C** and **F**) Urea content (C) and honeydew amino acid content (F) of *B. tabaci* post-RNAi. Gene-specific dsRNA (100 μg) of both *BtUCA* and *BtAtzF* was mixed into three different nitrogen contents, and the mixture was fed to insects for 96 hours. (**G**) Schematic representation of high-nitrogen stress assays in which *B. tabaci* adults were fed differently fertilized plants. To increase the nitrogen content of tobacco plants, the plants were without (0 mg) or with nitrogen fertilization (25 and 50 mg). Whiteflies that had been kept on no nitrogen–fertilized tobacco were transferred to the treated tobacco plants. (**H**, **J**, and **K**) The transcript levels of *BtUCA* (H) and *BtAtzF* (K) and the honeydew amino acid levels (J) after *B. tabaci* had fed a diet with different nitrogen levels for 4 days. (**I** and **L**) Urea content (I) and honeydew amino acid content (L) of *B. tabaci* post-RNAi after 9 days. Data are presented as mean values ± SEM; $n = 6$ (B, C, E, F, H, I, K, and L) biologically independent samples; ***$P < 0.001$; one-way ANOVA with Tukey's test was used for comparison.

## Involvement of *BtUCA* and *BtAtzF* in mitigating with high-nitrogen stress

To test the respective roles of *BtUCA* and *BtAtzF* in nitrogenous waste biosynthesis, the two abovementioned silencing approaches were also applied to confirm the roles of these genes in allowing the whiteflies to cope with high-nitrogen stress. In both cases, results from qPCR analyses showed that *BtUCA* and *BtAtzF* were significantly suppressed upon silencing (fig. S9, A to F). Silencing two genes via their diet more or less doubled urea levels in *B. tabaci* (Fig. 4C) and decreased the accumulations of amino acids in honeydew considerably (Fig. 4F). Knocking down both *BtUCA* and *BtAtzF* by having the whiteflies feed on cosilencing dsRNA-expressing transgenic tobacco plants also increased their urea contents, which was more than doubled (Fig. 4I and fig. S9G) and again significantly decreased the accumulations of amino acids in their honeydew (Fig. 4L and fig. S9H). This was the case for whiteflies that had been fed cosilencing transgenic tobacco plants for 5 or 9 days. Hence, both experiments showed that *BtUCA* and *BtAtzF* help the insect to adapt its nitrogen metabolism in accordance with the nitrogen levels in the diet.

## Activation of nitrogenous waste recycling during nitrogen deficiency

It has previously been shown that the amino acid and total nitrogen content is the same among *B. tabaci* individuals that are fed cotton plants with different nitrogen levels (*42*). It is also known that some

insects use nitrogen recycling to acquire nitrogen elements from stored inorganic nitrogen to overcome nitrogen deficiencies (*21*, *23*). As uricolytic enzymes play pivotal roles in nitrogen recycling (*17*) and *B. tabaci* MED encoded *BtUCA* and *BtAtzF*, we predicted that *B. tabaci* may also have evolved a nitrogen recycling ability. To confirm this, the effects of nitrogen deficiency stress on two species of whiteflies were investigated. Adults from laboratory-reared *B. tabaci* MED tobacco strain were randomly selected to feed on nitrogen-rich diet or nitrogen-deficient diet (Fig. 5A and fig. S11A). *B. tabaci* showed no difference in performance after feeding for 2 days (fig. S11, F and G) or 4 days (Fig. 5, F and G) on these diets, in terms of survival and reproduction. The free amino acid content of *B. tabaci* on the two diets was also not significantly different (Fig. 5E and fig. S11E). However, feeding on nitrogen-deficient diet significantly increased the expression levels of *BtUCA* and *BtAtzF* after 2 days (fig. S11C) or 4 days (Fig. 5C). Feeding on nitrogen-deficient diet also significantly increased the levels of *glutamate dehydrogenase* (*BtGDH*), *glutamine synthetase* (*BtGS*), *aspartate aminotransferase* (*BtaspC*), *branched-chain amino acid aminotransferase* (*BtilvE*), *diaminopimelate decarboxylase* (BtlysA), and *argininosuccinate lyase* (*BtargH*) after 2 or 4 days of feeding (fig. S12, A to F), as did the enzymatic activities of the BtUCA and BtAtzF proteins (fig. S11B and Fig. 5B). In contrast, feeding on nitrogen-deficient diet significantly reduced uric acid levels in *B. tabaci* (Fig. 5D and fig. S11D). These observations show that *B. tabaci* MED has an exceptional ability to recycle nitrogen when it is faced with insufficient nitrogen

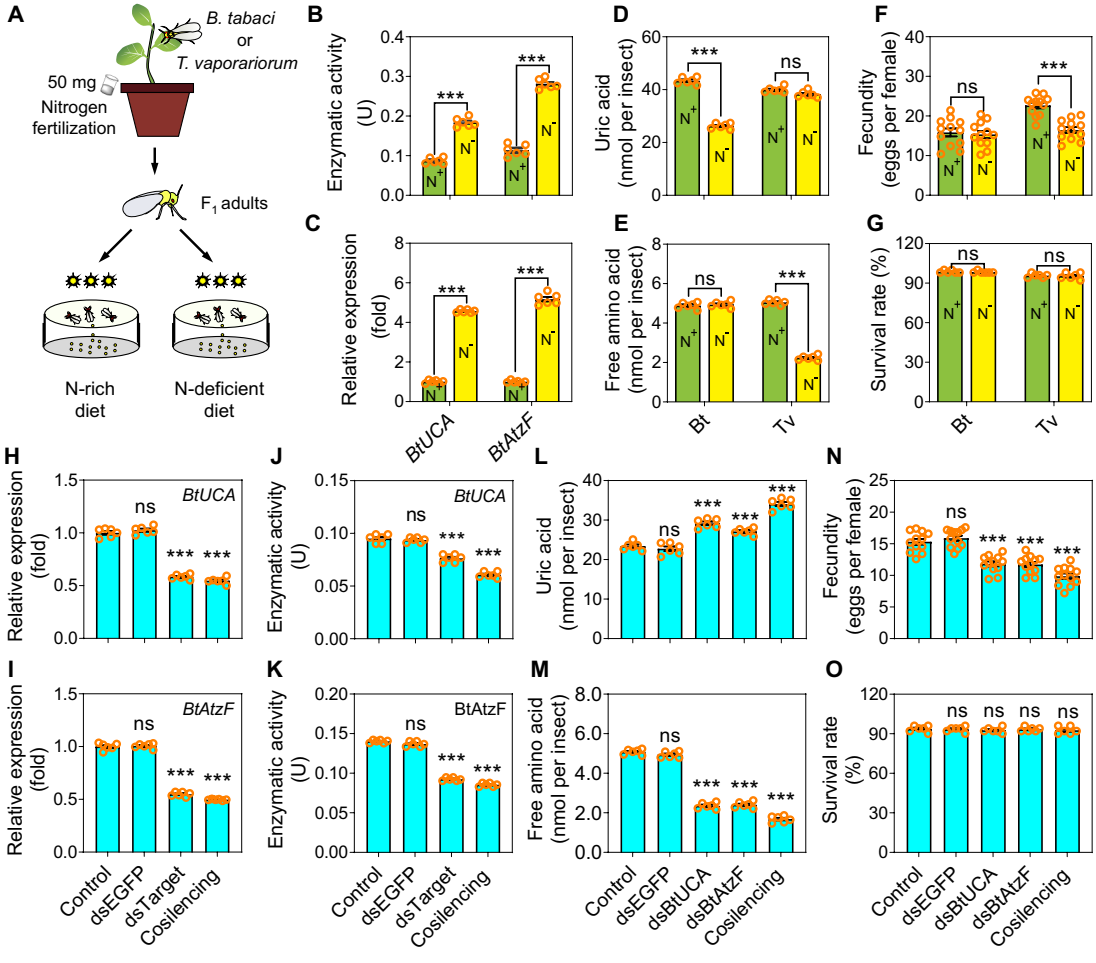


**Fig. 5. The role of *BtUCA* and *BtAtzF* in nitrogen recycling by *B. tabaci*.** (**A**) Schematic representation of nitrogen deficiency stress assays. Before investigating nitrogen recycling in *B. tabaci*, *B. tabaci* and *T. vaporariorum* were reared on wild-type tobacco plants with 50 mg of nitrogen fertilization for one generation. Newly emerged *B. tabaci* $F_1$ adults and *T. vaporariorum* $F_1$ adults were collected and placed on a nitrogen-rich diet (N-rich diet) (containing 5% yeast extract) or a nitrogen-deficient diet (N-deficient diet) (containing no yeast extract) for 96 hours. (**B**) Enzymatic activities of BtUCA and BtAtzF at 96 hours after feeding on diet with different nitrogen levels. (**C**) Transcript levels of *BtUCA* and *BtAtzF* at 96 hours after feeding on diet with different nitrogen levels. (**D** to **G**) Uric acid content (D), free amino acid content (E), fecundity (F), and survival rate (G) of *B. tabaci* (Bt) and *T. vaporariorum* (Tv) at 96 hours after feeding on diet with different nitrogen contents. (**H** to **K**) Transcript levels of *BtUCA* (H) and *BtAtzF* (I) and enzymatic activity of BtUCA (J) and BtAtzF (K) post-RNAi for 96 hours. (**L** to **O**) Uric acid content (L), free amino acid content (M), fecundity (N), and survival rate (O) of *B. tabaci* post-RNAi for 9 days. Nitrogen-rich diet labeled as $N^+$, and nitrogen-deficient diet labeled as $N^-$ (B to E). Data are presented as mean values ± SEM; $n = 6$ biologically independent samples; ***$P < 0.001$. Two-tailed Student's *t* test was used for comparison to generate *P* values in (B) to (G). One-way ANOVA with Dunnett's test was used for comparison in (H) to (O).

levels in its diet. *T. vaporariorum* was also tested in this study. Similar to *B. tabaci*, feeding on nitrogen-deficient diet did not affect *T. vaporariorum* survival (fig. S11G and Fig. 5G). In contrast to *B. tabaci*, in this related whitefly species, uric acid content was not affected by the different diets (fig. S11D and Fig. 5D) and free amino acid content and reproduction of *T. vaporariorum* significantly decreased when it fed the nitrogen-deficient diet (fig. S11E and Fig. 5, E and F). As *T. vaporariorum* does not have the two uricolytic enzymes UCA and AtzF, it may be unable to convert uric acid into amino acids (*17*, *21*, *23*); these differences between the insects of the *Bemisia* genus and *T. vaporariorum* further reinforce the notion that *B. tabaci* MED is inimitably able to recycle nitrogen.

### The role of *BtUCA* and *BtAtzF* in controlling nitrogen recycling

We then used RNAi to fully confirm that *BtUCA* and *BtAtzF* are involved in nitrogen recycling in *B. tabaci*. Upon silencing either *BtUCA* or *BtAtzF*, or both genes, their expression levels and enzymatic activities of their encoded proteins significantly decreased (Fig. 5, H to K, and fig. S11, H to K). The expression levels of *BtGDH*, *BtGS*, *BtaspC*, *BtilvE*, *BtlysA*, and *BtargH* were also significantly decreased in silenced *B. tabaci* after feeding for 2 or 4 days (fig. S12, G and H). Knocking down both *BtUCA* and *BtAtzF* did not significantly affect *B. tabaci* survival after 2 days (fig. S11O) or 4 days (Fig. 5O), but it significantly reduced its fecundity (Fig. 5N and fig. S11N). Silencing both genes also significantly inhibited uric acid degradation (Fig. 5L and fig. S11L) and reduced free amino acid content in honeydew (Fig. 5M and fig. S11M). In addition, the expression levels of some genes related to amino acid biosynthesis were also significantly affected after silencing (fig. S12, G and H). *BtGDH*, *BtGS*, and *BtaspC* serve in the biosynthesis of glutamate, which is the substrate for essential amino acids synthesis, and *BtilvE, BtlysA*, and *BtargH* mainly serve in the synthesis of the essential amino acids leucine, isoleucine, valine, lysine, and arginine (*43*, *44*). Therefore, the decreased expression level of these genes indicates that the essential amino acid biosynthesis was decreased in *B. tabaci* when the two HTGs were silenced. Moreover, ammonia is generated by *BtUCA* and *BtAtzF* and serves to provide amino groups in amino acid biosynthesis, implying that the two HTGs play a vital role in biosynthesizing amino acids for nitrogen recycling. The above results show that *BtUCA* and *BtAtzF* are involved in nitrogen recycling by *B. tabaci* MED.

### Involvement of *BtUCA* and *BtAtzF* in mitigating with low-nitrogen stress

Nitrogen recycling helps insects to overcome nitrogen shortages and enhanced their nutritional adaption (*21*, *45*). As nitrogen content in *B. tabaci*'s host plants can vary tremendously (*30*), we assumed that nitrogen recycling facilitates adaptation to distinct nitrogen levels during host plant switching. To investigate whether *BtUCA* and *BtAtzF* facilitate host adaptability in *B. tabaci*, we used hairpin RNA–expressing transgenic tobacco plants to achieve RNAi (Fig. 6A). The transcript levels of both genes were significantly reduced after the whitefly fed transgenic tobacco (Fig. 6, B and C, and fig. S13, C and D). In nonsilenced *B. tabaci*, switching to low-nitrogen plants significantly decreased uric acid content (Fig. 6D and fig. S13E), but did not significantly affect the free amino acid content, nor did it affect reproduction in *B. tabaci* (Fig. 6, E and F, and fig. S13, B and F). This was different when silencing both genes via the transformed tobacco plants. This resulted in significantly increased uric acid content (Fig. 6D and fig. S13E) and caused a significant decrease in amino acid content, as well as fecundity (Fig. 6, E and F, and fig. S13, B and F). Supplying some nitrogen improved fecundity and amino acid content of whitefly when *BtUCA* and *BtAtzF* were silenced (Fig. 6F and fig. S13B). The above observations imply that *BtUCA* and *BtAtzF* facilitate nitrogenous waste recycling and supply *B. tabaci* with amino acids and maintain the insects' reproductive capacity when the insects are faced with a nitrogen-deficient diet.

### Potential of silencing *BtUCA* and *BtAtzF* to control *B. tabaci*

Our last experiments were performed to investigate the potential of blocking *B. tabaci*'s nitrogenous waste processing ability as a control strategy against this global pest (Fig. 7A). *BtUCA* and *BtAtzF* were silenced in *B. tabaci* by feeding it on the above-described transgenic tobacco. Results showed that, upon silencing, the survival rate (Fig. 7B) and reproduction of *B. tabaci* $F_0$ adults (Fig. 7D) were significantly reduced. Although the survival rate and development time of *B. tabaci* $F_1$ eggs were not significantly affected, silencing both genes led to a significant reduction in survival rate and development time of $F_1$ nymphs (Fig. 7, F and H) and it also significantly reduced the fecundity of $F_1$ adults (Fig. 7J). In *T. vaporariorum*, which is closely related to *B. tabaci* but does not encode homologs of *BtUCA* and *BtAtzF*, none of these performance parameters were affected when feeding on the same transgenic tobacco (Fig. 7, C, E, G, I, and K). These latter results confirm that the genes are specific for *B. tabaci* and that a control approach with plant-mediated silencing will have no nontarget effects. Using transformed host plants to silence *BtUCA* and *BtAtzF*, possibly in combination with other silenced genes (*29*), has the potential to be an environmentally safe strategy for *B. tabaci* management.

## DISCUSSION

In animals, the biosynthesis of nitrogenous waste serves to reduce the accumulation of toxic nitrogen intermediates and even to store nitrogen for conservation and recycling. Most terrestrial insects export nitrogenous waste as uric acid (urate salt), but some terrestrial insects, especially sap-feeding insects, excrete nitrogen in the form of amino acids (*14*–*16*). Our current knowledge of nitrogenous waste biosynthesis in sap-feeding insects is very limited. Here, we show that *B. tabaci*, a well-known sap-feeding insect, has evolved a uniquely efficient and economic capacity to cope with nitrogenous waste with the help of two bacteria-derived genes (Fig. 8).

### *BtUCA* and *BtAtzF* mediate a low-cost nitrogenous waste biosynthesis in *B. tabaci*

As described above, unlike the majority of the extremely speciose terrestrial insects, sap-feeding insects excrete amino acid as waste. In most known cases, such as for the aphid *Acyrthosiphon pisum* and the planthopper *Nilaparvata lugens*, the biosynthesis of nitrogenous waste involves obligate symbionts (*16*, *46*). The transport of nitrogen-containing compounds, such as amino acids and nucleotides, across cells requires specific transporters (*47*, *48*) and comes with high energy costs for the insects (*49*), also when the biosynthesis is done by symbionts. By encoding the genes *BtUCA* and *BtAtzF*, *B. tabaci* does not have to depend on any symbionts for nitrogenous waste biosynthesis and, thus, the acquisition of these horizontally transferred genes has allowed *B. tabaci* to greatly reduce energetic costs.

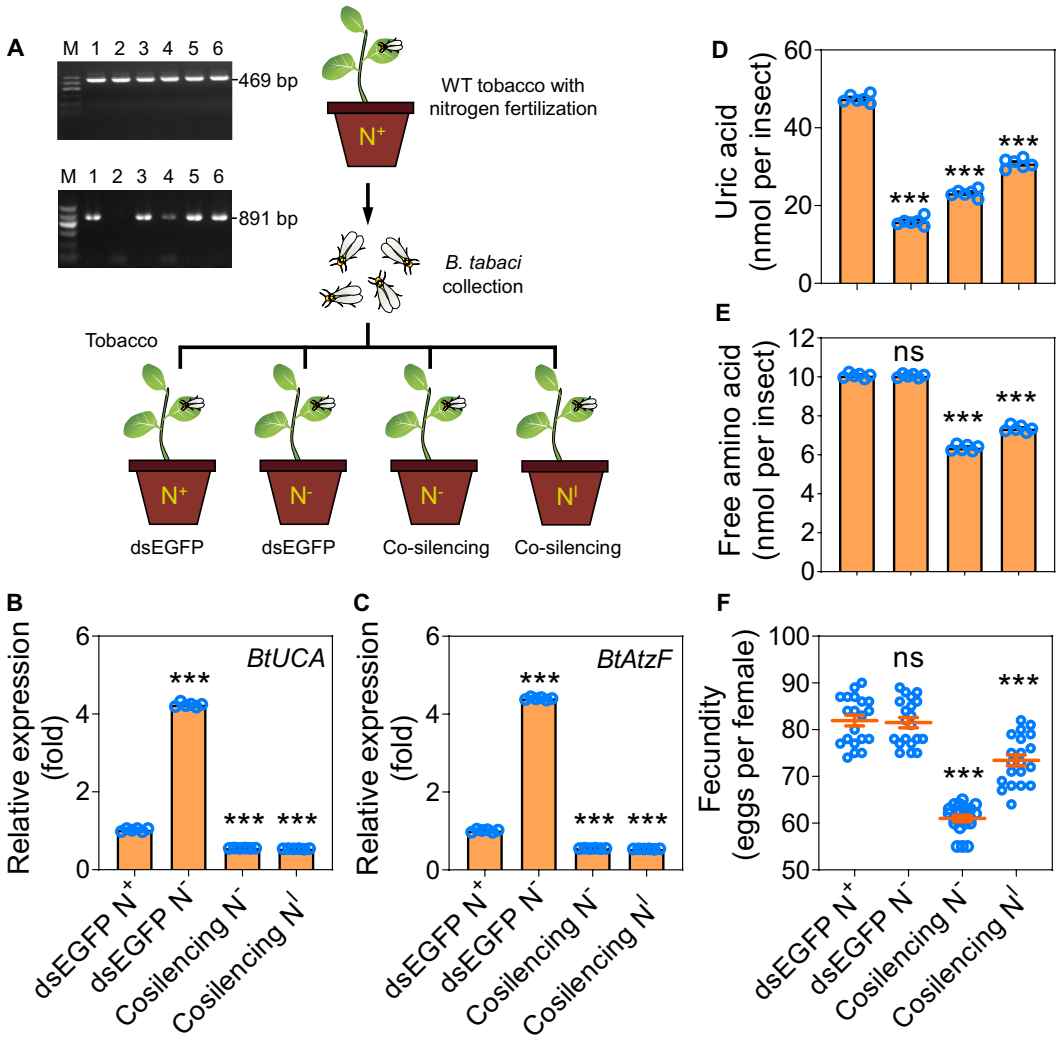


**Fig. 6. The importance of *BtUCA* and *BtAtzF* for host plant switching by *B. tabaci*.** (**A**) Schematic representation of host switching assays. *B. tabaci* $F_0$ was first reared on wild-type (WT) tobacco plants with nitrogen fertilization for one generation. The *B. tabaci* $F_1$ adults were switched to dsEGFP-expressing or cosilencing dsRNA-expressing transgenic tobacco. Electrophoresis figures represent the PCR analysis of transgenic tobacco plants. Top, EGFP-expressing transgenic tobaccos. M, marker (from top to bottom: 600 bp, 500 bp, 400 bp, 300 bp, 200 bp, 100 bp); lanes 1 to 6, EGFP-expressing transgenic tobaccos. Bottom, cosilencing dsRNA-expressing transgenic tobaccos. M, marker (from top to bottom: 1200 bp, 900 bp, 700 bp, 500 bp, 300 bp, 100 bp); lanes 1 to 6, putative cosilencing dsRNA-expressing transgenic tobacco plants. (**B** and **C**) Transcript levels of *BtUCA* (B) and *BtAtzF* (C) after *B. tabaci* $F_1$ adults had fed different transgenic tobacco plants for 9 days. (**D** to **F**) Uric acid levels (D), free amino acid content (E), and fecundity (F) of *B. tabaci* $F_1$ adults after feeding on different transgenic tobacco for 9 days. For all the figures, $N^+$ represents tobacco plants that received 50 mg of nitrogen fertilization. $N^-$ represents tobacco plants that received no nitrogen fertilization. $N^l$ represents tobacco plants that received only 10 mg of nitrogen fertilization. Data are presented as mean values ± SEM (B to E); $n = 6$ (B to E), $n = 20$ (F) biologically independent samples; ***$P < 0.001$; one-way ANOVA with Dunnett's test was used for comparison.

## Nitrogen recycling controlled by *BtUCA* and *BtAtzF* facilitates *B. tabaci*'s ability to adapt to its host plants

The intake of sufficient nitrogen is essential for all organisms. Nitrogen-based nutrition is also pivotal for insect performance (*32*), life span (*50*), and reproduction (*31*). Several insects are known to recycle nitrogen from their waste when faced with insufficient nitrogen in their diet. In cockroaches, termites, brown planthopper, oriental fruit fly, and turtle ants, waste recycling is regulated by obligated symbiont or gut bacteria (*21*, *23*, *45*, *51*). We found that the symbionts and gut bacteria of *B. tabaci* do not show any urea hydrolysis capacity, and therefore speculated that the bacteria-derived genes *BtUCA* and *BtAtzF* control nitrogen recycling in *B. tabaci* via a mechanism that is not dependent on microorganisms. We found that the two HTGs enable *B. tabaci* to conserve and acquire supplemental nitrogen when the insect was switched from high-nitrogen plants to low-nitrogen plants. *B. tabaci* feeds on an exceedingly wide range of host plants (*28*) that have largely varying amino acid contents (*30*). Our findings explain, at least in part, this ability to adapt to so many host plants. Nitrogen recycling not only is important for the development of feeding stages of insects but also is known to supply nitrogen for insect egg development (*23*), which explains why *BtUCA* and *BtAtzF* were found to also be highly expressed in the eggs. The flexible nitrogen recycling mechanism conferred by the two bacteria-derived genes might have facilitated *B. tabaci*'s invasiveness and spread as a worldwide pest.

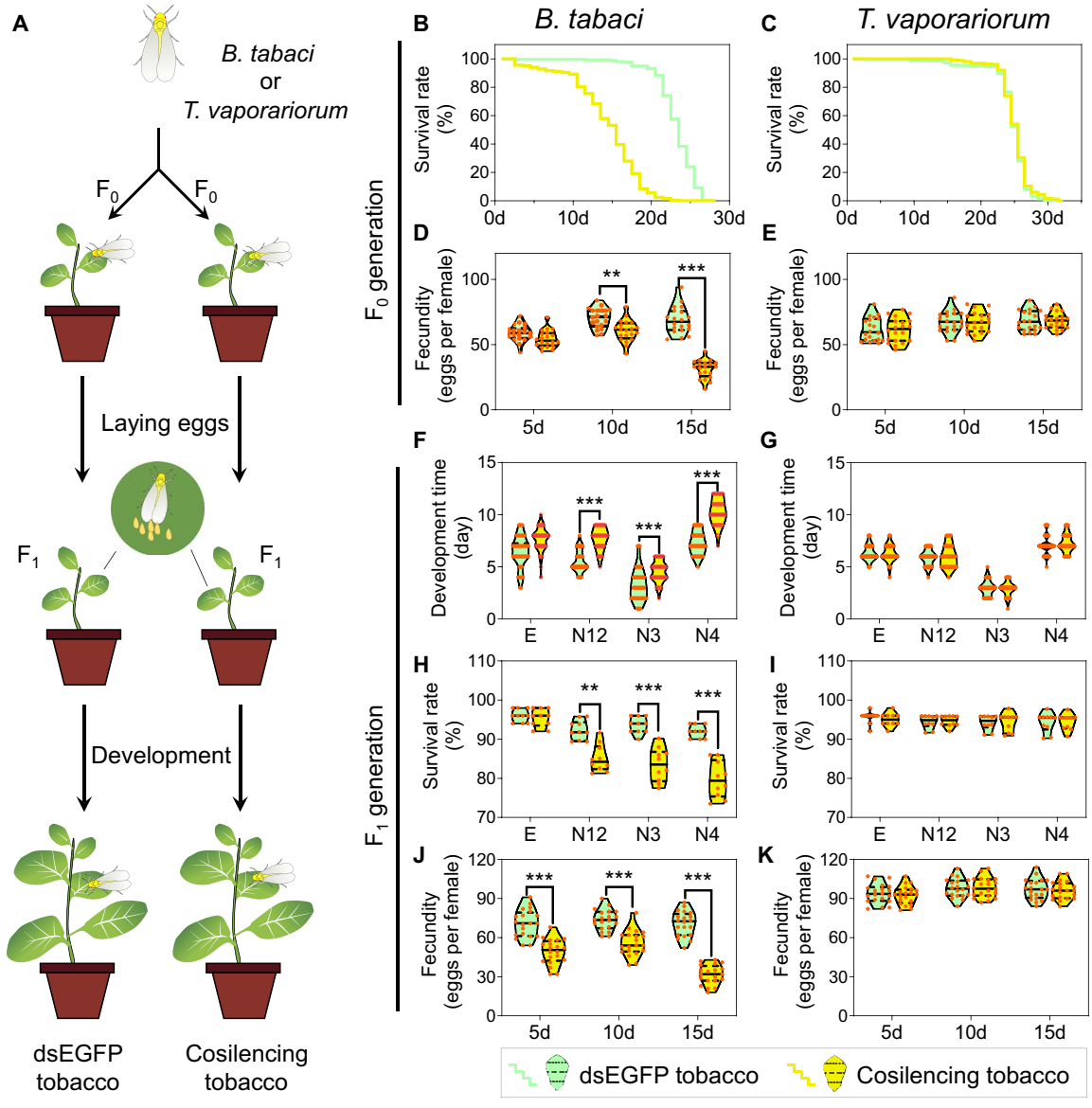


**Fig. 7. The importance of *BtUCA* and *BtAtzF* for *B. tabaci* performance.** (**A**) Schematic representation of the experimental design. Newly emerged *B. tabaci* $F_0$ and $F_1$ adults post-reproduction were reared on dsRNA-expressing transgenic tobacco plants. *T. vaporariorum* was used as a control. (**B** and **C**) Survival rate of *B. tabaci* $F_0$ (B) and *T. vaporariorum* $F_0$ (C) after rearing on dsRNA-expressing transgenic tobacco. (**D** and **E**) Fecundity (egg production) of *B. tabaci* $F_0$ (D) and *T. vaporariorum* $F_0$ (E) on days 5, 10, and 15 after rearing on dsRNA-expressing transgenic tobacco. (**F** and **G**) Total developmental time from egg to adult of *B. tabaci* $F_1$ nymph (F) and *T. vaporariorum* $F_1$ nymph (G) reared on dsRNA-expressing transgenic tobacco plants. (**H** and **I**) Survival rate of *B. tabaci* $F_1$ nymph (H) and *T. vaporariorum* $F_1$ nymph (I) reared on dsRNA-expressing transgenic tobacco plants. (**J** and **K**) Fecundity of *B. tabaci* $F_1$ (J) and *T. vaporariorum* $F_1$ (K) on days 5, 10, and 15 after rearing on dsRNA-expressing transgenic tobacco. In violin plots (D to K), box plots are included inside the plot. The center line represents median gene expression, and the dotted line spans the first quartile to the third quartile of the data distribution. Each violin plot is trimmed at the maximum and minimum value. $n = 5$ (B and C), $n = 10$ (H and I), $n = 20$ (D, E, J, and K), $n = 20$ (F and G) biologically independent samples. ***$P < 0.001$; two-tailed Student's $t$ test was used for comparison.

### *BtUCA* and *BtAtzF* provide insights into the importance of HTGs for the evolution of whiteflies

Horizontal gene transfer (HGT) is an important driving force for the adaptive evolution in prokaryotes and eukaryotes, especially in insects (*52*–*55*). The role of horizontally transferred genes (HTGs) in improving the adaptive capacity of recipient insects has been well documented (*56*, *57*). However, insect HTGs have rarely been reported to participate in and change insects' central metabolic processes. Here, we show that *BtUCA* and *BtAtzF* play such a role and account for a highly flexible and efficient exploitation of ingested nitrogen in whiteflies (Fig. 8). Hence, insect HTGs may carry out more essential tasks than previously recognized.

How such sophistication has evolved remains puzzling because HTGs can be expected to initially disrupt existing regulatory and physiological networks and potentially have major fitness costs for its recipients (*58*). This was likely also the case for *BtUCA* and

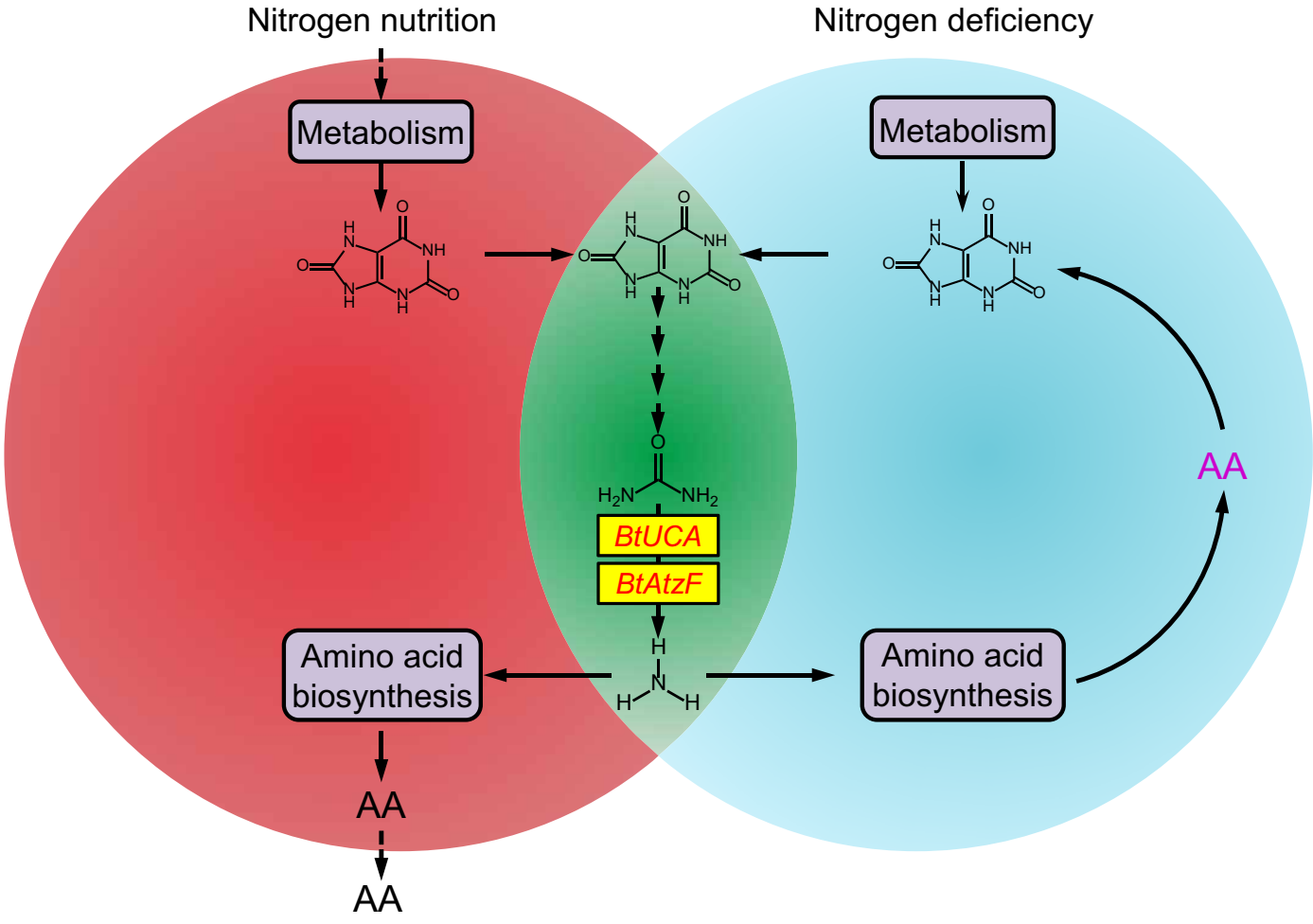


**Fig. 8. A proposed model for the central switch role of *BtUCA* and *BtAtzF* in the nitrogen metabolism of *B. tabaci*.** Urea that is generated from uric acid is converted by *BtUCA* and *BtAtzF* to ammonia. *BtUCA* and *BtAtzF* function to control nitrogenous waste biosynthesis as long as *B. tabaci* ingests sufficient N. The ammonia produced by the two HTGs is used to synthesize amino acid (AA) that is exported as nitrogenous waste. However, when *B. tabaci* is faced with insufficient nitrogen in its diet, *BtUCA* and *BtAtzF* serve to recycle nitrogen. The nitrogen elements recycled from uric acid by the two HTGs are again used to synthesize amino acid; this is supplied back to the insects.

*BtAtzF*. The tightly linked expression patterns of *BtUCA* and *BtAtzF* add to the mystery behind their evolutionary history and how it led to their integration in the same regulatory network of the whitefly. Whitefly populations can consist of exceedingly large numbers of individuals, and each whitefly individual carries millions of microorganisms. With such numbers, even the rarest of events, like HGT, will occur with such frequency that occasionally some of them will be favored by natural selection and eventually contribute to new traits that benefit the recipient species. In the rarest of cases, as we show here, it may even result in two HTGs operating in conjunction with each other. It is now clear that HGT has frequently occurred in eukaryotes with high population densities and generational turnover (*55*), but how recipients integrated HTGs, and specifically how the expression of different HTGs is regulated and how the recipients adapted to the metabolic changes caused by HTGs, has rarely been studied. For now, we can conclude that *BtUCA* and *BtAtzF* are an integral part of a metabolic pathway and share tightly related expression patterns. We also show that, because of the expression of *BtUCA* and *BtAtzF*, *B. tabaci* is able to overcome this deleterious effect by producing amino acids (fig. S12). Further investigations into the common features of *BtUCA* and *BtAtzF* may shed more light on how HTGs can be adopted and integrated by their recipients.

### *BtUCA* and *BtAtzF* may provide insight into the coevolution between insect hosts and their gut bacteria

Besides *B. tabaci*, our screens also revealed two urea-degrading HTGs, *urea amidolyases*, in the lacewing *Chrysoperla carnea* genome (*59*) (table S5). Previously, a urea-degrading HTG, another *urea amidolyases*, was also reported for the mealybug *Planococcus citri* (*60*). Many urea-degrading HTGs have been identified in a wide range of fungi (*61*), suggesting that different HGT events may have contributed to convergent evolution in both fungi and insects.

Various insects, like cockroaches (*21*), termites (*22*), *N. lugens* (*23*), and ants (*45*), depend on mutualistic relationships with their symbionts or gut bacteria to mediate nitrogen recycling. Here, we show that *B. tabaci* has acquired two functional bacteria-derived genes, through HGT, that participate in a unique process of the biosynthesis and recycling of nitrogenous waste. A urea-degrading HTG has also been reported for the mealybug *P. citri* (*60*). Because *P. citri* is another well-known sap-feeding insect and harbors obligate

symbionts that help them obtain essential amino acid, we speculate that, similar to *BtUCA* and *BtAtzF* in *B. tabaci*, urea-degrading HTGs in *P. citri* may also contribute to nitrogenous waste biosynthesis and nitrogen recycling. This would imply that the HGT may be of general evolutionary importance for sap-feeding insects, especially in mediating their nitrogenous waste cycling (Fig. 9).

A vast number of bacteria-derived HTGs have been reported for insects (*54*). Among them, a great number of these compensate for gene loss in obligate symbionts (*55*), especially in whitefly (*33*, *43*). It should be noted that we found no urea carboxylase or allophanate hydrolases in the obligate symbionts of *T. vaporariorum* or of whitefly species of the genus *Aleurodicus*, which implies that *BtUCA* and *BtAtzF* are unlikely to originate from obligate symbionts of *B. tabaci*, nor do they seem to compensate for a possible gene loss in such symbionts. Symbionts are not the only source of HTGs; several HTGs are also known to originate from gut bacteria (*53*, *55*). We therefore speculate that, before acquiring *BtUCA* and *BtAtzF*, *B. tabaci* relied on gut bacteria for its nitrogen metabolism, as is for instance the case for herbivorous turtle ants (*45*). As gut bacteria are unstable and easily affected by environmental changes (*62*), the HGT of *BtUCA* and *BtAtzF* may have endowed *B. tabaci* with a more stable and reliable nitrogen metabolism.

These types of HGT events are reminiscent of the Chinese idiom in the Analects of Confucius "Relying upon oneself is better than relying on others." Considering that no urea-degrading genes were identified in our meta-transcriptome analysis, we propose that *B. tabaci* has lost its urea-degrading bacteria after acquiring *BtUCA* and *BtAtzF*. Although further evidence is certainly needed, based on our findings, we speculate that HGT may be an important driving forcing in eliminating *B. tabaci's* reliance on mutualistic relationships with bacterial symbionts.

### *BtUCA* and *BtAtzF* are potential targets for pest management strategies

Failure to eliminate nitrogen intermediates can lead to cell damage and even cell death, as ammonia can be highly cytotoxic (*8*). Moreover, insufficient conversion and/or excretion of nitrogenous waste can cause pathological changes. For example, in humans, uric acid causes gout when it is not normally exported (*9*). Peroxynitrite attacks DNA and can lead to genome damage and cancers (*7*, *63*). Here, we also show that silencing *BtUCA* and *BtAtzF* in *B. tabaci* had highly unfavorable effects when it was fed tobacco supplied with nitrogen fertilization. This is expected when the whitefly is unable to eliminate toxic nitrogenous compounds. Nitrogen fertilization increases crop yield and is often an indispensable agricultural practice (*64*, *65*), but is known to benefit the performance of *B. tabaci* and can lead to outbreaks (*35*–*38*). Blocking nitrogenous waste biosynthesis in combination with nitrogen fertilization may have potential to control *B. tabaci*. As pest outbreaks resulting from nitrogen fertilization have been widely reported (*66*), interfering with nitrogenous waste biosynthesis could be a solution for other pests as well.

In brief, this study reveals that *B. tabaci* has acquired two bacterial genes, *BtUCA* and *BtAtzF*, that control the whitefly's highly efficient nitrogen cycling process. This insight into how *B. tabaci* copes with and exploits nitrogenous waste is particularly unique because it is a rare example of how two HTGs can evolve to work in tandem. Bacteria-derived HGT genes appear to be common in insects (*54*, *55*). Mining for more such genes in pest insects should provide further insights into how they have become so successful as pests and may reveal inspiring opportunities for the development of safe and efficient RNAi-based pest management strategies.

## MATERIALS AND METHODS

### Insect strains

The poinsettia strain of *B. tabaci* MED was collected from poinsettia (*Euphorbia pulcherrima* Wild. ex Klotz.) plant in Beijing in 2009, and it was subsequently transferred to cotton (*Gossypium herbaceum* L. cv. DP99B) to establish a cotton strain. The poinsettia strain was also transferred to tobacco (*Nicotiana tabacum* K326) to establish the tobacco strains in 2015. The cotton strain and tobacco strain had been reared on their respective host plants for over 100 generations and 45 generations, respectively, before being used in the experiments. The pepper strain was originally collected from cucumber plants in Beijing in 2011, and it was subsequently reared on pepper plants (*44*). Before being used in the experiments, this strain had been reared for over 80 generations on pepper. Two field samples of *B. tabaci* MED on tomato and eggplant plants were respectively collected in Shouguang, Shandong Province and Yuncheng, Shanxi Province in 2017 as previously described (*67*). Additionally, the greenhouse whitefly (*T. vaporariorum*) strain was provided by Y. Zhai at the Institute of Plant Protection, Shandong Academy of Agricultural Sciences, China in 2018, and it has been maintained on tobacco (*N. tabacum* K326) in our laboratory since then. All of the *B. tabaci* and *T. vaporariorum* strains were reared in an intelligence glasshouse at 27 ± 1°C, 60 to 80% relative humidity (RH), and 14-hour light/10-hour darkness.

### Metabolite profiling

A total weight of 131 μg of *B. tabaci* MED adults (about 2500 randomly mixed adults) from the laboratory-reared tobacco strain was collected and ground into powder in liquid nitrogen. The powder was solvent-extracted with 480 μl of methanol:chloroform (3:1, v/v). The extract was homogenized in a JXFSTPRP-24 tissue grinder (Shanghai Jingxin Technology) for 4 min at 45 Hz and ultrasonically treated for 5 min in ice water. This process was repeated three times. After centrifugation at 12,000*g* for 15 min, the supernatant was collected and dried using a TNG-T98 vacuum concentrator (Huamei Biochemical Instrument Factory). The dried supernatant was dissolved in 80 μl of methoxy amination hydrochloride (20 mg/ml in pyridine) and incubated for 30 min at 80°C. A total volume of 100 μl of the BSTFA [*N*,*O*-bis(trimethylsilyl)trifluoroacetamide] reagent containing 1% TMCS (trimethylchlorosilane; v/v) was added to the sample aliquots and incubated for 1.5 hours at 70°C. The extract was filtered through a 0.22-μm nylon membrane and stored at −20°C until use.

The extracts were analyzed using an Agilent 7890 gas chromatograph system equipped with a DB-5MS capillary column (30-m × 250-μm inner diameter, 0.25-μm film thickness; J&W Scientific) and coupled to a Pegasus HT time-of-flight mass spectrometer. Helium was used as the carrier gas, and the gas flow rate through the column was 1 ml per min. The temperature of the column was initially kept at 50°C for 1 min, increased to 310°C at a rate of 10°C min per min, and held for 5 min at 310°C. Injector temperature was 280°C, whereas the temperature of the transfer line and ion source was 280°C and 250°C, respectively. After 6.27 min (due to solvent delay), mass spectrometry (MS) data were acquired in full-scan mode at a rate of 20 spectra per second [mass/

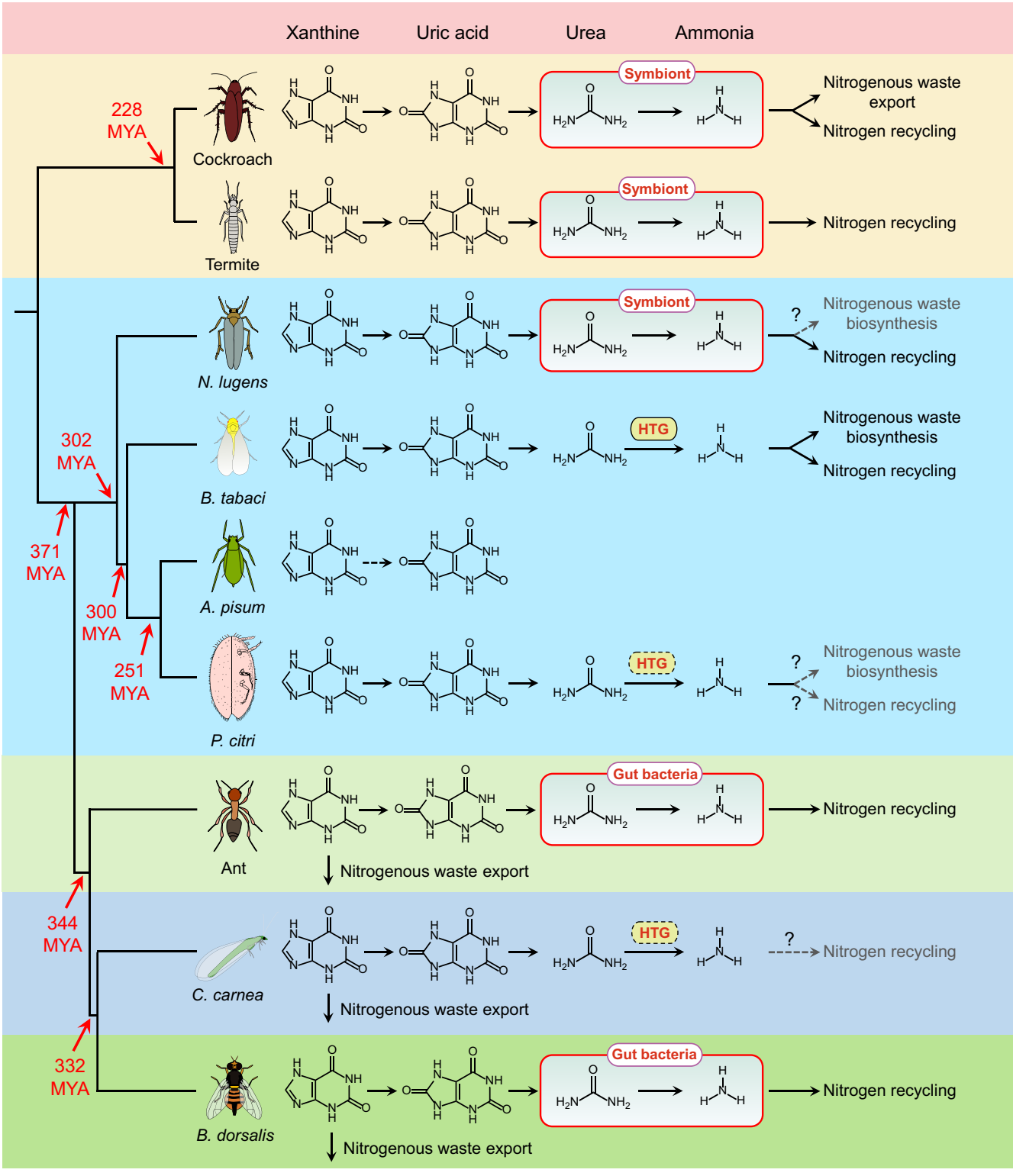


**Fig. 9. A comparison of nitrogenous waste biosynthesis and nitrogen recycling among different insects.** Schematic representation of nitrogen metabolism in various insects. Unlike the other insects, the unique nitrogen metabolism by *B. tabaci* relies on horizontal transferred genes from bacteria, and not on symbiont. The time scales of million years ago (MYA) presented the time when the insects diverged from each other (based on the TimeTree of Life, http://www.timetree.org/). The dotted lines and boxes with question marks represent tentative processes with no direct evidence.

charge ratio (*m/z*) range from 50 to 500]. Chroma TOF 4.3X software of LECO Corporation and LECO-Fiehn Rtx5 database were applied for metabolite identification by matching the mass spectrum and retention index (*68*).

### Isotope labeling experiment

To further confirm the nitrogenous waste biosynthesis that we predicted, an isotope labeling experiment was conducted. During the processes, a total amount of 69 μg of *B. tabaci* MED adults (about 1000 randomly mixed adults) was collected and reared in feeding dishes. The feeding dishes were placed in an MLR-352H environmental chamber (Panasonic) at 25°C and kept with a photoperiod of L14:D10 and 80% RH. Whitefly adults (freshly emerged within 24 hours) were fed an artificial diet, which contained 0.4% (w/v) $^{15}$N-labeled glutamic acid. After 3 days, the whiteflies and their honeydew were collected. Each whitefly sample was ground into powder in liquid nitrogen, and the powder was solvent-extracted with 90% methanol solution. After centrifugation at 12,000*g* for 15 min, the supernatant was collected. In addition, honeydew produced by the whiteflies was sampled and solvent-extracted with 90% methanol solution. After centrifugation at 12,000*g* for 15 min, the supernatant was collected. Each supernatant was filtered through a 0.22-μm nylon membrane and stored at −20°C until use.

### Measurements of $^{15}$N-labeled urea and amino acids

The $^{15}N_2$-labeled urea, $^{15}$N-labeled aspartic acid, $^{15}N_2$-labeled asparagine, and $^{15}N_2$-labeled glutamine were measured by liquid chromatography–MS (LC-MS) analysis. Before LC-MS analysis, the samples collected were diluted 100 times by 90% methanol solution. The chromatographic separations were performed on an Agilent 1290 Infinity LCsystem (Agilent Technologies). Analytes were separated on an Agilent InfinityLab Poroshell 120 HILIC-Z column (2.1 mm × 100 mm). The column and autosampler were maintained at 30°C and 4°C, respectively. The mobile phase was 10% ammonium formate buffer (pH 3.0; 200 mM, mobile phase A) and 10% ammonium formate buffer (pH 3.0; 200 mM) in acetonitrile (mobile phase B). The ultraperformance liquid chromatography (UPLC) separations were 20.5 min/sample using the following scheme: (i) 0 min, 100% B; (ii) 11.5 min, 70% B; (iii) 15 min, 50% B; (iv) 17 min, 50% B; (v) 17.5 min, 100% B; (vi) 20.5 min, 100% B. All the changes are linear, and the flow rate was set at 0.4 ml/min. Samples (2 μl) were injected for analysis by MS. Samples were analyzed by an Agilent 6495 triple-quadrupole mass spectrometer (Agilent Technologies) using positive electrospray ionization (ESI) and scheduled multiple reaction monitoring (MRM) mode. Settings were as follows: capillary voltage, +4.0 kV; nozzle voltage, 500 V; nitrogen was applied as a nebulizer gas of 35 psi, a carrier gas of 14 liters/min at 200°C, and a sheath gas of 12 liters/min at 250°C. MRM transitions, collision energies, and fragmentor voltages for $^{15}N_2$-labeled urea, $^{15}$N-labeled aspartic acid, $^{15}N_2$-labeled asparagine, and $^{15}N_2$-labeled glutamine were auto-optimized by Optimizer of Agilent MassHunter workstation.

### Sample collection, RNA extraction, and cDNA synthesis

Before investigating the expression profiles of *BtUCA* and *BtAtzF* via real-time quantitative PCR (qPCR), samples of different stages of *B. tabaci* MED were collected. During the processes, 2-day-old eggs, a mixture of first- and second-instar nymphs (after having hatched for 48 hours), and 1-day-old third-instar nymphs and 1-day-old fourth-instar nymphs of *B. tabaci* MED from laboratory-reared tobacco strain were collected. Different parts of *B. tabaci* MED adults were also collected. The *B. tabaci* MED adults, which emerged within 2 days, were collected. The heads, thoraxes, abdomens, and wings of collected adults were dissected. All the collected samples above were snap-frozen in liquid and used immediately or stored at −80°C until use.

Each sample was homogenized and extracted in TRIzol reagent (TaKaRa) according to the manufacturer's instruction. The RNA integrity was checked by 1% agarose gel electrophoresis, and the RNA concentration was measured using a NanoDrop2000c spectrophotometer (Thermo Fisher Scientific). The qualified RNA samples were used for meta-transcriptome sequencing, for cDNA synthesis for gene cloning, or for qPCR experiments. For gene cloning, the first-strand cDNA was synthesized with PrimeScript II first strand cDNA synthesis kit (TaKaRa). For qPCR, first-strand cDNA was synthesized using PrimeScript RT kit (containing gDNA Eraser, Perfect Real Time) (TaKaRa). Each synthesized cDNA sample was used immediately or stored at −20°C until use.

### Meta-transcriptome sequencing and analysis

To ensure that gut bacteria did not contribute to the biosynthesis of their host's nitrogenous waste, meta-transcriptome sequencing was applied for qualitative analyses. To obtain a global view of the contribution of gut bacteria to nitrogenous waste biosynthesis, four laboratory samples and two different geographical field samples were used. The laboratory samples included poinsettia, cotton, pepper, and tobacco strains of *B. tabaci* MED reared in our greenhouse as described above. For each sample, the total RNA of about 300 adults was extracted, purified, and quantified as described above. RNA-sequencing libraries were prepared using the TruSeq Stranded Total RNA Library Prep Kit with Ribo-Zero Gold (Illumina) following the manufacturer's instructions. Subsequently, the constructed libraries were quantified, normalized, and sequenced via Illumina HiSeq2500 platform. The obtained paired-end 2 × 150-bp (base pair) reads were deposited in the Sequence Read Archive (SRA; https://www.ncbi.nlm.nih.gov/sra) under the accession numbers SRR21290747 to SRR21290752.

Raw reads generated from each library were qualified and trimmed. To remove all the host-, endosymbiont-, and plant virus–derived reads, the clean reads were filtered out by mapping against genomes of *B. tabaci*, *B. tabaci* endosymbionts, and known plant viruses using Bowtie2 v2.3.5 (https://sourceforge.net/projects/bowtie-bio/files/bowtie2/2.3.5/) (table S4). The remaining reads were assembled using Trinity v2.8.5 (https://github.com/trinityrnaseq/trinityrnaseq/releases/tag/Trinity-v2.8.5). For each sample, the assembled transcripts were clustered and unigenes were filtered out. The finally obtained unigenes were used for microbial taxonomic classification and genetic capacity analysis. For microbial taxonomic identification, unigenes of each library were firstly blastp against the GenBank database (https://www.ncbi.nlm.nih.gov/). Taxonomic profiles of the unigenes were made based on the top hits. For genetic capacity analysis, unigenes were annotated with KOBAS 2.0 (http://kobas.cbi.pku.edu.cn/) and unigenes involved in final nitrogenous waste biosynthesis were picked out.

### Gene identification and cloning

To identify genes involved in nitrogenous waste metabolism in *B. tabaci*, the predicted gene sets of *B. tabaci* MED and its

endosymbionts were annotated by KOBAS 2.0. The predicted genes involved in final nitrogenous waste biosynthesis were picked out and rechecked by BLASTp against the GenBank database. The complete coding sequences of targeted genes were manually corrected with *B. tabaci* MED transcriptome assemble dataset (*44*). To clone the complete coding sequences of both *BtUCA* and *BtAtzF*, specific primer pairs (table S6) were designed by Primer Premier 5.0 (https://primer-premier-5.software.informer.com/). First-strand cDNA was synthesized using the PrimeScript II 1st strand cDNA Synthesis Kit. The PCRs were conducted using LA Taq polymerase with high GC buffer (TaKaRa). The detailed programs of PCR were listed below: denaturing at 94°C for 10 min; cycling 35 times with the following parameters: denaturing at 94°C for 60 s, annealing at 56° to 58°C (*BtUCA*, annealing at 56°C; *BtAtzF*, annealing at 58°C) for 60 s, and extension at 72°C for 2 to 4 min (*BtUCA*, extension for 4 min; *BtAtzF*, extension for 2 min); a final extension at 72°C for 10 min. The obtained amplicons of *BtUCA* and *BtAtzF* were purified, cloned into the pEASY-T1 vector (TransGen), and sequenced, and the finally obtained full-length cDNA sequences of both genes have been deposited in the GenBank database (*BtUCA*: GenBank accession no. ON513379; *BtAtzF*, GenBank accession no. ON513381).

### Phylogenetic analysis

For the phylogenetic tree construction, the amino acid sequences of *BtUCA* and *BtAtzF* genes were used as queries to identify homologs by BLASTp search in the GenBank database. As the amino acid sequences of both genes are highly conserved among closely related species, we only selected representative proteins from distantly related species to avoid redundancy. Those sequences were respectively aligned with MAFFT v7.311 using L-INS-I option (https://mafft.cbrc.jp/alignment/software). Before constructing the phylogenetic trees, the best protein substitution matrixes were predicted by Prottest V3.4.2 (https://github.com/ddarriba/prottest3). The alignments were used to infer the phylogenetic tree by MrBayes V3.2.3 (https://github.com/NBISweden/MrBayes/releases/tag/v3.2.3). For *BtAtzF*, the WAG + I + G + F protein substitution matrix was applied according to Prottest. For *BtUCA*, as the LG protein substitution matrix is not supported in MrBayes V3.2, phylogenies were inferred using a WAG + I + G + F protein substitution matrix. All the phylogenetic trees were displayed and annotated using iTol (https://itol.embl.de/).

### Bioinformatic analysis

A bioinformatics approach was used to confirm the incorporation of *BtUCA* and *BtAtzF* into the *B. tabaci* MED genome as previously described (*29*). In brief, paired-end Illumina genomic sequencing reads of *B. tabaci* MED, *B. tabaci* MEAM1, *B. tabaci* AsianII3, *B. tabaci* SSA, and *B. tabaci* NW were respectively mapped to the *B. tabaci* MED genome with Bowtie2 (*69*). Paired-end illumine transcriptome sequencing reads of *B. tabaci* MED, *B. tabaci* MEAM1, *B. tabaci* AsianII3, and *B. tabaci* SSA ployA selected RNA were also mapped to the genome of the *B. tabaci* MED. The alignments were sorted with samtools v1.7 (https://github.com/samtools/samtools/releases/tag/1.7) and visualized with IGV v2.5.3 (https://data.broadinstitute.org/igv/projects/downloads/2.5/). Coverages of each alignment were also calculated by IGV. To possibly identify homologs of both *BtUCA* and *BtAtzF* in *T. vaporariorum*, we used tblastn approaches (*70*).

### Genomic DNA isolation and cloning

A total number of 100 *B. tabaci* MED adults from the laboratory-reared tobacco strain was collected and ground into a powder in liquid nitrogen. Their genomic DNA (gDNA) was isolated using the TIANamp Genomic DNA Kit (TIANGEN) following the manufacturer's instructions. The DNA integrity was checked by 1% agarose gel electrophoresis, and the DNA concentration was measured using a NanoDrop2000c spectrophotometer (Thermo Fisher Scientific). On the basis of the *B. tabaci* MED genome sequences, specific primers were designed by Primer Premier 5.0 to amplify the intergenic genomic regions of the *BtUCA*, *BtAtzF*, and their neighboring genes. Amplicons of each PCR were purified, cloned into the pEASY-T1 vector, and sequenced.

### qPCR analysis

The expression levels of target genes were quantified using the QuantStudio 3 Real-Time PCR System (Applied Biosystems). On the basis of the obtained coding sequences of *BtUCA* and *BtAtzF*, specific primer pairs of both genes (table S6) were designed by Primer Premier 5.0. The amplification specificity of primer pairs was confirmed by the occurrence of a single peak in a melting curve following qPCR. The amplification efficiencies of primers were 90% to 110%. Each primer pair with proper amplification specificity and efficiency was used in qPCRs with 2.5 × SYBR Green MasterMix Kit (TIANGEN). Three-step qPCR programs were applied. Besides annealing temperatures (*BtUCA*, 59°C; *BtAtzF*, 58°C), other parameters of qPCR program followed the manufacturer's instructions. Primer pairs of amino acid synthesis genes were designed and selected, and qPCR experiments were conducted as described above. For relative quantification, *elongation factor 1*α (*EF1*-α) (GenBank accession no. EE600682) was selected as a reference gene. The relative expression level of each gene was calculated according to the $2^{-\Delta\Delta Ct}$ method (*71*).

### Heterologous expression and protein purification

To estimate the catalytic activity of *BtUCA* and *BtAtzF*, the recombinant proteins were heterologously expressed in *E. coli* BL21. Coding sequences of both genes were respectively subcloned into the pET28a vector. The two recombinant vectors were separately transformed into *E. coli* BL21. Single positive transformed colonies were selected and sequenced. Later, the corrected single positive transformed colony of each gene was incubated overnight at 37°C in 5 ml of LB medium [containing kanamycin (100 μg/ml)]. A total volume of 1 ml of each incubation was individually added to a 100-ml LB medium [containing kanamycin (100 μg/ml)] and incubated at 37°C. Isopropyl β-D-thiogalactopyranoside (IPTG) solution (0.5 mM, Solarbio) was added to LB culture when $OD_{600}$ (optical density at 600 nm) of culture reached 0.1. The incubation was grown at 20°C, 120 rpm for 4.5 hours before harvesting by centrifugation at 3000*g* for 5 min at 4°C. The pellets were thawed and dissolved in 4 ml of phosphate-buffered saline (PBS) buffer [pH 7.4, containing 1 mM phenylmethylsulfonyl fluoride (PMSF)]. After incubating with lysozyme (Solarbio) for 60 min, cell debris was removed by centrifugation for 20 min at 12,000*g* at 4°C and the supernatant was collected. The two recombinant proteins were further purified using Amicon Pro Purification System (Millipore). Briefly, the proteins were eluted with buffer A (50 mM tris-HCl, 200 mM NaCl, and imidazole gradient ranging from 50 to 250 nM,

pH 8.3). To remove imidazole, each elution was added to a HiTrap desalting column (GE Healthcare) with buffer B (50 mM tris-HCl, pH 8.3). Finally, ultrafiltration of the recombinant proteins was performed with a 30-kDa cutoff Amicon Ultra-0.5 Device (Millipore). The final purified recombinant proteins were mixed with a 5 × SDS loading buffer, separated by SDS–polyacrylamide gel electrophoresis (PAGE) (BtUCA, 10% acrylamide gel; BtAtzF, 12% acrylamide gel), and stained with 0.1% Coomassie blue R-250 in water.

### Enzyme activity assays

The kinetic assays of the recombinant proteins BtUCA and BtAtzF were performed at 25°C in a Spectra M2$^e$ (Molecular Devices) microplate reader. The kinetic assay of BtUCA was performed as described in a previous study (*40*). In brief, the reaction mixture contained 50 mM Hepes buffer, 50 mM KCl, 8 mM $MgSO_4$, 1 mM ATP, 1.5 mM phosphoenolpyruvate, 8 mM $KHCO_3$, 0.15 mM NADPH (reduced form of nicotinamide adenine dinucleotide phosphate), urea at different concentrations, 10 U of pyruvate kinase (Solarbio), 25 U of lactate dehydrogenase (Solarbio), and 1 μg of BtUCA. The BtUCA activity was monitored spectrophotometrically by coupling the adenosine diphosphate (ADP)–forming reaction with the reactions catalyzed by pyruvate kinase and lactate dehydrogenase. The reaction was determined at 340 nm. One unit of enzyme activity was defined as 1 μM nicotinamide adenine dinucleotide (NAD) formed per minute.

Before performing the kinetic assay with BtAtzF, potassium allophanate was synthesized using ethyl allophanate (Sigma-Aldrich) and quantified based on a previous study (*41*). The kinetic assay of BtAtzF was performed as described elsewhere (*72*). The reaction mixture comprised 100 mM tris-HCl, 1 μM EDTA, 3 mM $MgCl_2$, 19.5 mM potassium chloride, 200 U of glutamate dehydrogenase (GLDH) (Solarbio), 50 mM oxoglutaric acid, 0.3 mM NADPH, potassium allophanate at different concentrations, and 1 μg of BtAtzF. The BtAtzF activity was measured by coupling ammonium release to NADH [reduced form of nicotinamide adenine dinucleotide (oxidized form)] to NAD conversion through GLDH. The reaction was determined at 340 nm, and 1 U of enzyme activity was defined as 1 μM NAD formed per minute.

### dsRNA preparation for RNAi by direct feeding

To investigate the roles of *BtUCA* and *BtAtzF* in *B. tabaci*, an RNAi approach by feeding them dsRNA via an artificial diet was first applied. The dsRNA of each gene was synthesized as follows. On the basis of the coding sequence of *BtUCA* and *BtAtzF*, gene-specific primers including a T7 promoter sequence (table S6) for dsRNA synthesis were designed by Primer Premier 5.0. A 476-bp fragment of *BtUCA* and a 461-bp fragment of *BtAtzF* were respectively cloned for dsRNA synthesis. To avoid potential off-target effects, we further did a BLASTn search of the designed dsRNA fragments in the GenBank and *B. tabaci* genome databases, and no hits to any other homologous genes were detected, further confirming the dsRNA specificity. The dsRNA of each gene was synthesized with T7 RiboMAX Express RNAi system (Promega) according to the manufacturer's instructions. The dsRNA of *enhanced green fluorescent protein* (*EGFP*) gene (GenBank accession no. KC896843) was synthesized and used as the negative control. The thus different generated dsRNAs were used in feeding assays with an artificial diet (see below).

### Preparation of VIGS plants for RNAi

VIGS assays were also used to explore the role of *BtUCA* and *BtAtzF* in *B. tabaci* nitrogenous waste. Virus vectors for VIGS have been described previously (*29*). The experimental process is shown in Fig. 3H. A 453-bp fragment of *BtUCA* and a 438-bp fragment of *BtAtzF* were respectively cloned via specific primer pairs (table S6). The amplicons were respectively cloned into Eco RI–Bam HI–cut pTRV2 to construct pTRV2-dsBtUCA and pTRV2-dsBtAtzF. Next, the amplicons were also tandemly inserted into Eco RI–Bam HI–cut pTRV2 to construct pTRV2-cosilencing vector with the In-Fusion HD Cloning Kit (TaKaRa) following the manufacturer's instructions. A 469-bp fragment of the *EGFP* gene (GenBank accession no. KC896843) was cloned using specific primers (table S6), and the PCR product was cloned into Eco RI–Bam HI–cut pTRV2 to construct pTRV2-EGFP. The pTRV1, pTRV2-dsBtUCA, pTRV2-dsBtAtzF, and pTRV2-cosilencing vectors were separately transferred into *Agrobacterium tumefaciens* GV3101 by electroporation. LB agar plates [rifampicin (100 μg/ml), kanamycin (50 μg/ml)] were used to screen for positive clones, and the clones were validated by PCR amplification.

The *A. tumefaciens* GV3101 harboring pTRV1 or pTRV2 with the desired fragment was added to 5 ml of liquid LB medium [rifampicin (100 μg/ml) and kanamycin (50 μg/ml)]. The cultures were incubated at 28°C, 200 rpm shaking and kept for 18 hours. Then, 4-ml volume of each culture was added to 96-ml flesh liquid LB medium [rifampicin (100 μg/ml), kanamycin (50 μg/ml), 200 μM acetosyringone, and 10 mM MES]. The cultures were later incubated at 28°C, shaken at 200 rpm, and kept for 18 hours. Later, the bacterium was harvested by centrifuging the culture at 3000*g* for 10 min. The pellets were washed using an infiltration medium (200 μM acetosyringone, 10 mM MES, and 10 mM $MgCl_2$). Finally, all bacterial strains were resuspended in an infiltration medium until their $OD_{600}$ reached 0.4. Each GV3101 containing pTRV2 with the desired fragment was mixed with an equal volume of GV3101 containing pTRV1. The mixtures were injected into the two largest leaves of tobacco (*N. tabacum* K326) using a 1-ml needleless syringe. The tobacco plants were kept in an MLR-352H environmental chamber (Panasonic) at 25 ± 1°C, 70 ± 10% RH, at a photoperiod of L16:D8. After 3 weeks, PCR was performed to determine whether the VIGS vectors were successfully infected with VIGS-specific primers (table S6). The infected tobacco plants were selected for further study.

### Preparation of hairpin RNA–expressing transgenic tobacco plants for RNAi

The third RNAi approach to investigate the true importance of *BtUCA* and *BtAtzF* involved hairpin RNA–expressing transgenic tobacco. To create the transgenic tobacco lines, we introduced the hairpin RNA expression vector (pCAMBIA-RNAi-cosilencing) into *N. tabacum* K326 plants. A fragment of *BtUCA* and *BtAtzF* was respectively cloned from *B. tabaci* MED using specific primers (table S6). The purified PCR product was tandemly inserted into Xho I–Bgl II–cut pCAMBIA-RNAi and reversely tandemly inserted into Bam HI–Sal I–cut pCAMBIA-RNAi. The constructed pCAMBIA-RNAi-cosilencing vector was transformed into *A. tumefaciens* GV3101 by electroporation. The *A. tumefaciens* GV3101-based transformation was used to transfer the constructed plasmid into tobacco. To verify the success of the transformation, gDNA of putative transgenic tobacco leaves was extracted using the Plant Genomic DNA Kit (TIANGEN), and the extracted gDNA was subjected to

PCR using detection primers (table S6). The selected $T_0$ transgenic tobacco plants were allowed to self-fertilize. The $T_1$ transgenic tobacco plants were selected by kanamycin (50 mg/liter) containing germination medium and PCR verification. Later, the selected $T_1$ transgenic tobacco plants were allowed to self-fertilize. The homozygous transgenic tobacco plants were filtered out by germination medium [containing kanamycin (50 mg/liter)] and PCR verification.

### Feeding assays with dsRNA to investigate the roles of *BtUCA* and *BtAtzF* in nitrogenous waste biosynthesis

To confirm the importance of *BtUCA* and *BtAtzF* in processing nitrogen in *B. tabaci*, we first studied their involvement in producing nitrogenous waste using the dsRNA feeding RNAi approach. The assays were performed as described previously (*29*). Feeding dishes (see Fig. 3C) were placed in an MLR-352H environmental chamber (Panasonic) at 25°C and with a photoperiod of L14:D10 and 80% RH. Whitefly adults (freshly emerged within 24 hours) were fed an artificial diet, which was supplemented with the dsRNA of only *BtUCA*, of only *BtAtzF,* or of both genes. The two control treatments involved diet without dsRNA or dsRNA of *EGFP*. Each treatment involved 300 *B. tabaci* adults from the laboratory-reared tobacco strain. After feeding for 4 days, the adult whiteflies were collected and the expression levels of targeted genes and urea contents were measured. In addition, we measured the levels of free amino acids in the whiteflies' honeydew. Each experiment was replicated six times.

### VIGS plant–mediated RNAi to investigating the roles of *BtUCA* and *BtAtzF* in nitrogenous waste biosynthesis

To further investigate the role of *BtUCA* and *BtAtzF* in *B. tabaci* nitrogenous waste biosynthesis, the second abovementioned RNAi approach (via VIGS plants) was applied. This involved feeding the whiteflies in cages on the generated VIGS plants, again silencing one of the two genes or both. Control plants were either not transformed or transformed with a fragment of the *EGFP* gene, as described above. Each treatment involved 350 *B. tabaci* adults from the laboratory-reared tobacco strain. After feeding for 3, 5, 7, and 9 days, the adult whiteflies were collected and their expression levels of targeted genes and urea contents were measured. The contents of free amino acid in the whiteflies' waste were also assessed. Each experiment was replicated six times.

### High-nitrogen stress assay

After confirming the unique nitrogenous waste biosynthesis mechanism in *B. tabaci*, we also investigated how high-nitrogen stress affected the biosynthetic process. In a first series of experiments, whitefly adults (freshly emerged within 24 hours) were fed a sucrose solution (30% sucrose, w/v) containing different levels of nitrogen (2.5% yeast extract, 5% yeast extract, and 10% yeast extract). The yeast extract was purchased from OXOID (LP0021), which contains 5.1% amino nitrogen. The feeding experiment was conducted in feeding chambers using the dsRNA-feeding RNAi approach (Fig. 4A). Each treatment contained 350 *B. tabaci* adults from the laboratory-reared tobacco strain. After feeding for 1, 2, 3, and 4 days, the whitefly adults were collected and the content of amino acids in their honeydew was determined. The expression levels of *BtUCA* and *BtAtzF* were assessed by qPCR. In addition, a series of isotope labeling experiments was conducted to further study the products resulting from nitrogenous waste biosynthesis in *B. tabaci* MED under high-nitrogen stress. Whitefly adults (freshly emerged within 24 hours) were fed a sucrose solution (30% sucrose, w/v) containing different levels of nitrogen (0.2% yeast extract + 0.1% $^{15}$N-labeled glutamic acid, 0.2% yeast extract + 0.2% $^{15}$N-labeled glutamic acid, and 0.2% yeast extract + 0.4% $^{15}$N-labeled glutamic acid, w/v). The feeding experiments were conducted in feeding chambers as described above. For each treatment, we used 350 *B. tabaci* adults from the laboratory-reared tobacco strain. After feeding for 2 and 4 days, the whitefly adults were collected and the $^{15}N_2$-labeled asparagine and $^{15}N_2$-labeled glutamine contents in their honeydew were determined. The expression levels of *BtUCA* and *BtAtzF* were also assessed by qPCR.

In a second series of experiments, tobacco plants were supplied with different levels of fertilization (0, 25, and 50 mg) and 350 newly emerged (within 2 days) whitefly adults reared on tobacco without nitrogen fertilization were collected and placed into clip cages. The clip cages were fixed on leaves of the differently treated tobacco plants (Fig. 4G). After feeding for 3, 5, 7, and 9 days, the whitefly adults were collected and the content of amino acids in their honeydew was determined. The expression levels of *BtUCA* and *BtAtzF* were also assessed by qPCR.

### Determining the roles of *BtUCA* and *BtAtzF* in mitigating the effects of high-nitrogen stress

After confirming that high-nitrogen stress promotes nitrogenous waste biosynthesis in *B. tabaci*, we next investigated the roles of *BtUCA* and *BtAtzF* in mitigating high-nitrogen stress, using the two described RNAi approach (via dsRNA-feeding and hairpin RNA–expressing transgenic tobacco plants). In dsRNA-feeding approach, the dsRNA of *BtUCA* and *BtAtzF* was synthesized as described above. *B. tabaci* MED adults (freshly emerged within 24 hours) were fed with different nitrogen-containing (2.5% yeast extract, 5% yeast extract, and 10% yeast extract) sucrose solution (30% sucrose, w/v) with or without the two dsRNAs. The feeding experiments were also conducted in feeding chambers as RNAi treatments. Each treatment contained 350 *B. tabaci* adults from the laboratory-reared tobacco strain. After feeding for 4 days, the whitefly adults were collected. The urea content of *B. tabaci* adults and amino acid content in the whiteflies' honeydew was determined. The expression levels of *BtUCA* and *BtAtzF* were assessed by qPCR. Each experiment was replicated six times. In all the assays, the dsRNA of EGFP used as the negative control and whitefly adults fed a sucrose solution without dsRNA were used as controls.

For RNAi assays with hairpin RNA–expressing transgenic tobacco plant, the dsEGFP-expressing and cosilencing transgenic tobacco plants were supplied with different levels of fertilization (0, 25, and 50 mg). A number of 350 newly emerged (within 2 days) whitefly adults reared on wild-type tobacco without nitrogen fertilization were collected and placed into clip cages. The clip cages were fixed on leaves of the differently treated tobacco plants. After feeding for 5 and 9 days, the whitefly adults were collected. The urea content of *B. tabaci* adults and the content of amino acids in their honeydew were determined. The expression levels of *BtUCA* and *BtAtzF* were assessed by qPCR. Each experiment was replicated six times. In all the assays, the whitefly adults fed dsEGFP-expressing tobacco plants were used as the negative control and whitefly adults fed wild-type tobacco plants were used as controls.

### Urea and uric acid concentration measurements

For each sample, 100 *B. tabaci* MED adults were collected. The collected whiteflies were immediately frozen in liquid nitrogen and stored at −80°C until use. Urea concentration in each sample was assessed using the Urea Assay Kit (Colorimetric, Abcam) following the manufacturer's protocols. For each test, 50 *B. tabaci* MED adults were homogenized to determine urea concentration. Uric acid concentration in each sample was assessed using the Micro Uric Acid (UA) Content Assay Kit (Solarbio) following the manufacturer's protocols.

### Honeydew collection and amino acid quantification

Honeydew in feeding chambers and clip cages was collected as previously described (*29*). After collection, each sample was immediately frozen in liquid nitrogen and stored at −80°C until use. The honeydew samples were dissolved in 800 μl of methanol, and after centrifuging the solution at 12,000*g* for 15 min, the supernatant was collected and dried. The dried supernatant was dissolved in 150 μl of Extracted Buffer (Solarbio) to measure free amino acid concentrations using the Micro Amino Acid (AA) Content Assay Kit (Solarbio) according to the manufacturer's instructions.

### Nitrogen deficiency stress assays

Next, we investigated if *BtUCA* and *BtAtzF* help *B. tabaci* to recycle nitrogen under nitrogen deficiency stress. Before determining the whitefly's nitrogen recycling capacity, the effects of nitrogen deficiency stress on *B. tabaci* were measured. First, nearly 1000 *B. tabaci* adults and *T. vaporariorum* from the laboratory-reared tobacco strain were reared on wild-type tobacco with standard nitrogen fertilization (50 mg per plant) for one generation. The newly emerged (within 24 hours) whitefly adults were collected and transferred to feeding chambers, where they were fed with either a nitrogen-rich artificial diet (5% yeast extract and 30% sucrose, w/v) or a nitrogen-deficient diet (30% sucrose, w/v). These feeding treatments were also performed for RNAi assays, as above. Each treatment involved 350 *B. tabaci* adults from the laboratory-reared tobacco strain. Adults were collected after feeding on the different diets for 48 and 96 hours. After RNAi silencing, 50 whitefly adults were used for qPCR, 100 whitefly adults were used to assess uric acid content, and 200 whitefly adults were used to determine amino acid content. To measure fecundity, 80 whitefly females (freshly emerged within 24 hours) were similarly fed an artificial diet of different nitrogen levels in the feeding chambers. After feeding for 48 and 96 hours on these diets, five whitefly females were randomly collected and placed in one clip cage and that was attached to a tobacco leaf. After 3 days, the numbers of whitefly eggs they had laid on the leaves were recorded.

### Determining the roles of *BtUCA* and *BtAtzF* in nitrogen recycling

The importance of *BtUCA* and *BtAtzF* for nitrogen recycling was further investigated by feeding *B. tabaci* MED $F_1$ adults (reared on 50 mg of nitrogen-fertilized tobacco and freshly emerged within 24 hours) with a nitrogen-free artificial diet (30% sucrose, w/v) with or without the two different types of dsRNA. As described above, the experiments were performed in feeding chambers, and each treatment involved about 430 whiteflies. The *B. tabaci* MED adults were collected after feeding on the different diets for 48 and 96 hours. After silencing, 40 whitefly adults were used for qPCR, 80 whitefly adults were used to measure enzymatic activity, 100 whitefly adults were used to access uric acid content, and 200 whitefly adults were used to determine amino acid content. For fecundity measurements, 80 whitefly females (freshly emerged within 24 hours) were fed with the different types of artificial diets in feeding chambers. After feeding for 48 and 96 hours, five whitefly females per treatment were randomly collected and placed in a clip cage attached to a tobacco leaf for 3 days. The number of eggs they had laid was recorded. In all the assays, the whitefly adults fed dsEGFP-expressing tobacco plants were used as the negative control and whitefly adults fed wild-type tobacco plants were used as standard controls.

### Free amino acid quantification

For each sample, 200 *B. tabaci* MED adults of a particular treatment were collected. The collected whiteflies were immediately frozen in liquid nitrogen and stored at −80°C until use. For each test, the collected whiteflies were homogenized and extracted in in 150 μl of Extracted Buffer (Solarbio). After centrifuging the solution at 3000*g* for 5 min, the supernatant was collected, which was used to measure free amino acid concentrations using the Micro Amino Acid (AA) Content Assay Kit (Solarbio) according to the manufacturer's instructions.

### Host switching assays

The importance of *BtUCA* and *BtAtzF* in allowing *B. tabaci* to switch between host plants with distinctly different nitrogen contents was further investigated. To avoid the differences in anti-insect response among different plants, we used tobacco plants that received different nitrogen fertilization regimes. Before performing the experiment, nearly 1000 *B. tabaci* adults from the laboratory-reared tobacco strain were fed wild-type tobacco with standard nitrogen fertilization (50 mg per plant) for one generation. The newly emerged (within 24 hours) whitefly $F_1$ adults were placed into clip cages and reared on differently treated transgenic tobacco plants. The four treatments included dsEGFP transgenic tobacco plants with or without nitrogen fertilization (50 mg per tobacco), as well as cosilencing transgenic tobacco plants with or without nitrogen fertilization (10 mg per tobacco). To determine the impact of *BtUCA* and *BtAtzF* on gene expression levels, enzymatic activity, uric acid content, and free amino acid content, an additional clip cage experiment was performed. Because of the size limitations of the clip cages, each treatment involved eight clip cages, with about 60 whitefly adults each. After feeding for 3, 5, 7, and 9 days, the whitefly adults were collected. Fifty whitefly adults were used for qPCR, and 80 whitefly adults were collected to measure enzymatic activity. A total of 100 whitefly adults were used to assess uric acid content, and 200 whitefly adults were used to determine amino acid content. In each case, there were six biological replicates. To determine the impact of *BtUCA* and *BtAtzF* on whitefly reproduction, we conducted an additional experiment for which five newly emerged whitefly females were placed in single clip cages. Each clip cage was fixed on treated transgenic tobacco plants. After rearing for 3, 5, 7, and 9 days, the numbers of whitefly eggs on the plants were recorded. Each experiment involved 20 biological replicates. In all the assays, whitefly adults feeding on dsEGFP-expressing tobacco plants without nitrogen fertilization were used as the negative control and whitefly adults feeding on dsEGFP-expressing tobacco plants with nitrogen fertilization were used as standard controls.

### RNAi-based *B. tabaci* control

A series of experiments was conducted to investigate the potential of silencing *BtUCA* and *BtAtzF* in *B. tabaci* for pest management. To determine the lethal effects of *BtUCA* and *BtAtzF* silencing on *B. tabaci* $F_0$ adults, 20 newly emerged (within 2 days) whitefly adults from the laboratory-reared tobacco strain were placed in a clip cage and fixed on a leaf of a dsEGFP transgenic tobacco plant or of a co-silencing transgenic tobacco plant. The survival of whitefly adults in each clip cage was recorded every day. A total of six biological replicates were used for this experiment. To determine the effects of *BtUCA* and *BtAtzF* on *B. tabaci* $F_0$ reproduction, five newly emerged (within 2 days) whitefly females were placed in one clip cage and fixed on a dsEGFP transgenic tobacco plant or a cosilencing transgenic tobacco plant. The number of eggs that they laid was recorded every 5 days. Because of the lethal effects of silencing *BtUCA* and *BtAtzF*, only the first 15 days were recorded. To determine the effects of silencing *BtUCA* and *BtAtzF* on *B. tabaci* $F_1$ nymph survival and development, 20 newly emerged (within 2 days) whitefly females were placed in a clip cage and fixed on different treated tobacco plants. After 2 days, the whitefly eggs were counted. The developmental period and survival rate of the $F_1$ were recorded. In addition, to determine the effects of silencing *BtUCA* and *BtAtzF* on *B. tabaci* $F_1$ adult reproduction, five newly emerged (within 2 days) whitefly $F_1$ females were placed in a clip cage and fixed on a dsEGFP or a cosilencing transgenic tobacco plant. Again, egg production was recorded every 5 days for a total of 15 days. Similar to *B. tabaci*, efforts of silencing *BtUCA* and *BtAtzF* on the *T. vaporariorum* $F_0$ and *T. vaporariorum* $F_1$ were also determined. For all experiments, 20 biological replicates were used, and in all cases, the plants were fertilized with nitrogen (50 mg per plant) every 5 days.

### Statistical analysis

All the data were analyzed using the IBM SPSS Statistics (ver. 23.0) software (IBM Corp.). Data are shown as means ± SEM. For pairwise comparisons, the data statistical significance was determined using Student's *t* test. For multiple comparisons, the data statistical significance was determined using one-way analysis of variance (ANOVA) with Tukey's test or Dunnett's test, as indicated in the figure legends. Significance was reported as $*P < 0.05$, $**P < 0.01$, $***P < 0.001$.

## Supplementary Materials

**This PDF file includes:**

Figs. S1 to S13
Tables S2 to S6
Legends for tables S1 and S7

**Other Supplementary Material for this manuscript includes the following:**

Tables S1 and S7

## REFERENCES AND NOTES


1. G. Xu, X. Fan, A. J. Miller, Plant nitrogen assimilation and use efficiency. *Annu. Rev. Plant Biol.* **63**, 153–182 (2012).
2. K.-E. Chen, H.-Y. Chen, C.-S. Tseng, Y.-F. Tsay, Improving nitrogen use efficiency by manipulating nitrate remobilization in plants. *Nat. Plants* **6**, 1126–1135 (2020).
3. G. Wu, F. W. Bazer, Z. Dai, D. Li, J. Wang, Z. Wu, Amino acid nutrition in animals: Protein synthesis and beyond. *Annu. Rev. Anim. Biosci.* **2**, 387–417 (2014).
4. Q. Lin, C. Ané, T. J. Givnish, S. W. Graham, A new carnivorous plant lineage (*Triantha*) with a unique sticky-inflorescence trap. *Proc. Natl. Acad. Sci. U.S.A.* **118**, e2022724118 (2021).
5. J. Kim, K. L. Guan, mTOR as a central hub of nutrient signalling and cell growth. *Nat. Cell Biol.* **21**, 63–71 (2019).
6. M. Neinast, D. Murashige, Z. Arany, Branched chain amino acids. *Annu. Rev. Physiol.* **81**, 139–164 (2019).
7. E. W. Gerner, F. L. Meyskens Jr., Polyamines and cancer: Old molecules, new understanding. *Nat. Rev. Cancer* **4**, 781–792 (2004).
8. D. C. Hess, W. Lu, J. D. Rabinowitz, D. Botstein, Ammonium toxicity and potassium limitation in yeast. *PLOS Biol.* **4**, e351 (2006).
9. K. L. Rock, H. Kataoka, J. J. Lai, Uric acid as a danger signal in gout and its comorbidities. *Nat. Rev. Rheumatol.* **9**, 13–23 (2013).
10. R. Keshet, P. Szlosarek, A. Carracedo, A. Erez, Rewiring urea cycle metabolism in cancer to support anabolism. *Nat. Rev. Cancer* **18**, 634–645 (2018).
11. J. Linden, F. Koch-Nolte, G. Dahl, Purine release, metabolism, and signaling in the inflammatory response. *Annu. Rev. Immunol.* **37**, 325–347 (2019).
12. P. A. Wright, Nitrogen excretion: Three end products, many physiological roles. *J. Exp. Biol.* **198**, 273–281 (1995).
13. D. E. Mullins, D. G. Cochran, Nitrogen excretion in cockroaches: Uric acid is not a major product. *Science* **177**, 699–701 (1972).
14. D. N. Byrne, W. B. Miller, Carbohydrate and amino acid composition of phloem sap and honeydew produced by *Bemisia tabaci*. *J. Insect Physiol.* **36**, 433–439 (1990).
15. T. Sasaki, T. Aoki, H. Hayashi, H. Ishikawa, Amino acid composition of the honeydew of symbiotic and aposymbiotic pea aphids *Acyrthosiphon pisum*. *J. Insect Physiol.* **36**, 35–40 (1990).
16. T. Sasaki, M. Kawamura, H. Ishikawa, Nitrogen recycling in the brown planthopper, *Nilaparvata lugens*: Involvement of yeast–like endosymbionts in uric acid metabolism. *J. Insect Physiol.* **42**, 125–129 (1996).
17. Z. L. Sabree, S. Kambhampati, N. A. Moran, Nitrogen recycling and nutritional provisioning by *Blattabacterium*, the cockroach endosymbiont. *Proc. Natl. Acad. Sci. U.S.A.* **106**, 19521–19526 (2009).
18. J. M. Wiebler, K. D. Kohl, R. E. Lee, J. P. Costanzo, Urea hydrolysis by gut bacteria in a hibernating frog: Evidence for urea-nitrogen recycling in Amphibia. *Proc. R. Soc. B* **285**, 20180241 (2018).
19. G. Cui, Y. J. Liew, Y. Li, N. Kharbatia, N. I. Zahran, A. H. Emwas, V. M. Eguiluz, M. Aranda, Host-dependent nitrogen recycling as a mechanism of symbiont control in Aiptasia. *PLOS Genet.* **15**, e1008189 (2019).
20. M. D. Regan, E. Chiang, Y. Liu, M. Tonelli, K. M. Verdoorn, S. R. Gugel, G. Suen, H. V. Carey, F. M. Assadi-Porter, Nitrogen recycling via gut symbionts increases in ground squirrels over the hibernation season. *Science* **375**, 460–463 (2022).
21. D. E. Mullins, Physiology of environmental adaptations and resource acquisition in cockroaches. *Annu. Rev. Entomol.* **60**, 473–492 (2015).
22. A. Brune, Symbiotic digestion of lignocellulose in termite guts. *Nat. Rev. Microbiol.* **12**, 168–180 (2014).
23. A. E. Douglas, Multiorganismal insects: Diversity and function of resident microorganisms. *Annu. Rev. Entomol.* **60**, 17–34 (2015).
24. S.-S. Liu, P. J. De Barro, J. Xu, J.-B. Luan, L.-S. Zang, Y.-M. Ruan, F.-H. Wan, Asymmetric mating interactions drive widespread invasion and displacement in a whitefly. *Science* **318**, 1769–1772 (2007).
25. P. J. De Barro, S. S. Liu, L. M. Boykin, A. B. Dinsdale, *Bemisia tabaci*: A statement of species status. *Annu. Rev. Entomol.* **56**, 1–19 (2011).
26. X. W. Wang, S. Blanc, Insect transmission of plant single-stranded DNA viruses. *Annu. Rev. Entomol.* **66**, 389–405 (2021).
27. R. G. Jain, S. J. Fletcher, N. Manzie, K. E. Robinson, P. Li, E. Lu, C. A. Brosnan, Z. P. Xu, N. Mitter, Foliar application of clay-delivered RNA interference for whitefly control. *Nat. Plants* **8**, 535–548 (2022).
28. M. R. V. Oliveira, T. J. Henneberry, P. Anderson, History, current status, and collaborative research projects for *Bemisia tabaci*. *Crop Prot.* **20**, 709–723 (2001).
29. J. Xia, Z. Guo, Z. Yang, H. Han, S. Wang, H. Xu, X. Yang, F. Yang, Q. Wu, W. Xie, X. Zhou, W. Dermauw, T. C. J. Turlings, Y. Zhang, Whitefly hijacks a plant detoxification gene that neutralizes plant toxins. *Cell* **184**, 1693–1705.e17 (2021).
30. X. Jiao, W. Xie, S. Wang, Q. Wu, L. Zhou, H. Pan, B. Liu, Y. Zhang, Host preference and nymph performance of B and Q putative species of *Bemisia tabaci* on three host plants. *J. Pest Sci.* **85**, 423–430 (2012).
31. C. S. Awmack, S. R. Leather, Host plant quality and fecundity in herbiborous insects. *Annu. Rev. Entomol.* **47**, 817–844 (2002).
32. W. C. Wetzel, H. M. Kharouba, M. Robinson, M. Holyoak, R. Karban, Variability in plant nutrients reduces insect herbivore performance. *Nature* **539**, 425–427 (2016).
33. F.-R. Ren, X. Sun, T.-Y. Wang, Y.-L. Yao, Y.-Z. Huang, X. Zhang, J.-B. Luan, Biotin provisioning by horizontally transferred genes from bacteria confers animal fitness benefits. *ISME J.* **14**, 2542–2553 (2020).
34. F. R. Ren, X. Sun, T.-Y. Wang, J.-Y. Yan, Y.-L. Yao, C.-Q. Li, J.-B. Luan, Pantothenate mediates the coordination of whitefly and symbiont fitness. *ISME J.* **15**, 1655–1667 (2021).
35. J.-A. Bentz, J. Reeves III, P. Barbosa, B. Francis, Nitrogen fertilizer effect on selection, acceptance, and suitability of *Euphorbia pulcherrima* (Euphorbiaceae) as a host plant to *Bemisia tabaci* (Homoptera: Aleyrodidae). *Environ. Entomol.* **24**, 40–45 (1995).

36. J. L. Bi, G. R. Ballmer, D. L. Hendrix, T. J. Henneberry, N. C. Toscano, Effect of cotton nitrogen fertilization on *Bemisia argentifolii* populations and honeydew production. *Entomol. Exp. Appl.* **99**, 25–36 (2001).
37. L. Hilje, H. S. Costa, P. A. Stansly, Cultural practices for managing *Bemisia tabaci* and associated viral diseases. *Crop Prot.* **20**, 801–812 (2001).
38. J.-L. Bi, D.-M. Lin, K.-S. Lii, N. C. Toscano, Impact of cotton planting date and nitrogen fertilization on *Bemisia argentifolii* populations. *Insect Sci.* **12**, 31–36 (2005).
39. D. Santos-Garcia, C. Vargas-Chavez, A. Moya, A. Latorre, F. J. Silva, Genome evolution in the primary endosymbiont of whiteflies sheds light on their divergence. *Genome Biol. Evol.* **7**, 873–888 (2015).
40. T. Kanamori, N. Kanou, H. Atomi, T. Imanaka, Enzymatic characterization of a prokaryotic urea carboxylase. *J. Bacteriol.* **186**, 2532–2539 (2004).
41. T. Kanamori, N. Kanou, S. Kusakabe, H. Atomi, T. Imanaka, Allophanate hydrolase of *Oleomonas sagaranensis* involved in an ATP-dependent degradation pathway specific to urea. *FEMS Microbiol. Lett.* **245**, 61–65 (2005).
42. S. J. Crafts-Brandner, Plant nitrogen status rapidly alters amino acid metabolism and excretion in *Bemisia tabaci*. *J. Insect Physiol.* **48**, 33–41 (2002).
43. J.-B. Luan, W. Chen, D. K. Hasegawa, A. M. Simmons, W. M. Wintermantel, K.-S. Ling, Z. Fei, S.-S. Liu, A. E. Douglas, Metabolic coevolution in the bacterial symbiosis of whiteflies and related plant sap-feeding insects. *Genome Biol. Evol.* **7**, 2635–2647 (2015).
44. W. Xie, C. Chen, Z. Yang, L. Guo, X. Yang, D. Wang, M. Chen, J. Huang, Y. Wen, Y. Zeng, Y. Liu, J. Xia, L. Tian, H. Cui, Q. Wu, S. Wang, B. Xu, X. Li, X. Tan, M. Ghanim, B. Qiu, H. Pan, D. Chu, H. Delatte, M. N. Maruthi, F. Ge, X. Zhou, X. Wang, F. Wan, Y. du, C. Luo, F. Yan, E. L. Preisser, X. Jiao, B. S. Coates, J. Zhao, Q. Gao, J. Xia, Y. Yin, Y. Liu, J. K. Brown, X. J. Zhou, Y. Zhang, Genome sequencing of the sweetpotato whitefly *Bemisia tabaci* MED/Q. *GigaScience* **6**, 1–7 (2017).
45. Y. Hu, J. G. Sanders, P. Łukasik, C. L. D'Amelio, J. S. Millar, D. R. Vann, Y. Lan, J. A. Newton, M. Schotanus, D. J. C. Kronauer, N. E. Pierce, C. S. Moreau, J. T. Wertz, P. Engel, J. A. Russell, Herbivorous turtle ants obtain essential nutrients from a conserved nitrogen-recycling gut microbiome. *Nat. Commun.* **9**, 964 (2018).
46. I. Liadouze, G. Febvay, J. Guillaud, G. Bonnot, Effect of diet on the free amino acid pools of symbiotic and aposymbiotic pea aphids, *Acyrthosiphon pisum*. *J. Insect Physiol.* **41**, 33–40 (1995).
47. K. Sawada, N. Echigo, N. Juge, T. Miyaji, M. Otsuka, H. Omote, A. Yamamoto, Y. Moriyama, Identification of a vesicular nucleotide transporter. *Proc. Natl. Acad. Sci. U.S.A.* **105**, 5683–5686 (2008).
48. H. Feng, N. Edwards, C. M. H. Anderson, M. Althaus, R. P. Duncan, Y. C. Hsu, C. W. Luetje, D. R. G. Price, A. C. C. Wilson, D. T. Thwaites, Trading amino acids at the aphid–*Buchnera* symbiotic interface. *Proc. Natl. Acad. Sci. U.S.A.* **116**, 16003–16011 (2019).
49. P. Kandasamy, G. Gyimesi, Y. Kanai, M. A. Hediger, Amino acid transporters revisited: New views in health and disease. *Trends Biochem. Sci.* **43**, 752–789 (2018).
50. K. M. Hoedjes, M. A. Rodrigues, T. Flatt, Amino acid modulation of lifespan and reproduction in *Drosophila*. *Curr. Opin. Insect Sci.* **23**, 118–122 (2017).
51. X. Ren, S. Cao, M. Akami, A. Mansour, Y. Yang, N. Jiang, H. Wang, G. Zhang, X. Qi, P. Xu, T. Guo, C. Niu, Gut symbiotic bacteria are involved in nitrogen recycling in the tephritid fruit fly *Bactrocera dorsalis*. *BMC Biol.* **20**, 201 (2022).
52. S. M. Soucy, J. Huang, J. P. Gogarten, Horizontal gene transfer: Building the web of life. *Nat. Rev. Genet.* **16**, 472–482 (2015).
53. B. J. Arnold, I. T. Huang, W. P. Hanage, Horizontal gene transfer and adaptive evolution in bacteria. *Nat. Rev. Microbiol.* **20**, 206–218 (2022).
54. Y. Li, Z. Liu, C. Liu, Z. Shi, L. Pang, C. Chen, Y. Chen, R. Pan, W. Zhou, X.-X. Chen, A. Rokas, J. Huang, X.-X. Shen, HGT is widespread in insects and contributes to male courtship in lepidopterans. *Cell* **185**, 2975–2987.e10 (2022).
55. F. Husnik, J. P. McCutcheon, Functional horizontal gene transfer from bacteria to eukaryotes. *Nat. Rev. Microbiol.* **16**, 67–79 (2018).
56. N. Wybouw, Y. Pauchet, D. G. Heckel, T. Van Leeuwen, Horizontal gene transfer contributes to the evolution of arthropod herbivory. *Genome Biol. Evol.* **8**, 1785–1801 (2016).
57. A. Prasad, O. Chirom, M. Prasad, Insect herbivores benefit from horizontal gene transfer. *Trends Plant Sci.* **26**, 1096–1097 (2021).
58. D. A. Baltrus, Exploring the costs of horizontal gene transfer. *Trends Ecol. Evol.* **28**, 489–495 (2013).
59. L. Crowley, University of Oxford and Wytham Woods Genome Acquisition Lab, Darwin Tree of Life Barcoding collective, Wellcome Sanger Institute Tree of Life programme, Wellcome Sanger Institute Scientific Operations: DNA Pipelines collective, Tree of Life Core Informatics collective, Darwin Tree of Life Consortium, The genome sequence of the common green lacewing, *Chrysoperla carnea* (Stephens, 1836). *Wellcome Open Res.* **6**, 334 (2021).
60. F. Husnik, N. Nikoh, R. Koga, L. Ross, R. P. Duncan, M. Fujie, M. Tanaka, N. Satoh, D. Bachtrog, A. C. C. Wilson, C. D. von Dohlen, T. Fukatsu, J. P. McCutcheon, Horizontal gene transfer from diverse bacteria to an insect genome enables a tripartite nested mealybug symbiosis. *Cell* **153**, 1567–1578 (2013).
61. P. K. Strope, K. W. Nickerson, S. D. Harris, E. N. Moriyama, Molecular evolution of urea amidolyase and urea carboxylase in fungi. *BMC Evol. Biol.* **11**, 80 (2011).
62. P. Brinker, M. C. Fontaine, L. W. Beukeboom, J. F. Salles, Host, symbionts, and the microbiome: The missing tripartite interaction. *Trends Microbiol.* **27**, 480–488 (2019).
63. R. A. Casero Jr., T. Murray Stewart, A. E. Pegg, Polyamine metabolism and cancer: Treatments, challenges and opportunities. *Nat. Rev. Cancer* **18**, 681–695 (2018).
64. X. Zhang, E. A. Davidson, D. L. Mauzerall, T. D. Searchinger, P. Dumas, Y. Shen, Managing nitrogen for sustainable development. *Nature* **528**, 51–59 (2015).
65. Z. Cui, H. Zhang, X. Chen, C. Zhang, W. Ma, C. Huang, W. Zhang, G. Mi, Y. Miao, X. Li, Q. Gao, J. Yang, Z. Wang, Y. Ye, S. Guo, J. Lu, J. Huang, S. Lv, Y. Sun, Y. Liu, X. Peng, J. Ren, S. Li, X. Deng, X. Shi, Q. Zhang, Z. Yang, L. Tang, C. Wei, L. Jia, J. Zhang, M. He, Y. Tong, Q. Tang, X. Zhong, Z. Liu, N. Cao, C. Kou, H. Ying, Y. Yin, X. Jiao, Q. Zhang, M. Fan, R. Jiang, F. Zhang, Z. Dou, Pursuing sustainable productivity with millions of smallholder farmers. *Nature* **555**, 363–366 (2018).
66. P. Han, A. V. Lavoir, C. Rodriguez-Saona, N. Desneux, Bottom-up forces in agroecosystems and their potential impact on arthropod pest management. *Annu. Rev. Entomol.* **67**, 239–259 (2022).
67. H. Zheng, W. Xie, B. Fu, S. Xiao, X. Tan, Y. Ji, J. Cheng, R. Wang, B. Liu, X. Yang, Z. Guo, S. Wang, Q. Wu, B. Xu, X. Zhou, Y. Zhang, Annual analysis of field-evolved insecticide resistance in *Bemisia tabaci* across China. *Pest Manag. Sci.* **77**, 2990–3001 (2021).
68. T. Kind, G. Wohlgemuth, D. Y. Lee, Y. Lu, M. Palazoglu, S. Shahbaz, O. Fiehn, FiehnLib: Mass spectral and retention index libraries for metabolomics based on quadrupole and time-of-flight gas chromatography/mass spectrometry. *Anal. Chem.* **81**, 10038–10048 (2009).
69. X. Li, P. Liang, M. Wu, S. Wang, Q. Wu, W. Xie, Y. Zhang, Several whitefly genome assemblies and an integrated whitefly gene search platform. *Insect Sci.*, (2023).
70. W. Xie, C. He, Z. Fei, Y. Zhang, Chromosome-level genome assembly of the greenhouse whitefly (*Trialeurodes vaporariorum* Westwood). *Mol. Ecol. Resour.* **20**, 995–1006 (2020).
71. K. J. Livak, T. D. Schmittgen, Analysis of relative gene expression data using real-time quantitative PCR and the $2^{-\Delta\Delta CT}$ method. *Methods* **25**, 402–408 (2001).
72. C. Fan, Z. Li, H. Yin, S. Xiang, Structure and function of allophanate hydrolase. *J. Biol. Chem.* **288**, 21422–21432 (2013).


**Acknowledgments:** We thank W. Dermauw from the Flanders Research Institute for Agriculture, Fisheries and Food (ILVO), Belgium for his invaluable comments on an early version of this study. We thank the public laboratory of the Biotechnology Research Institute, Chinese Academy of Agricultural Sciences for the use of the HPLC and triple-quadrupole MS/MS instrument and for providing technical assistance. **Funding:** This research was supported by the National Key R&D Program of China (grant no. 2021YFD1400600 to Z.G.), National Natural Science Foundation of China (grant nos. 32221004 to Y.Z., 32102216 to Z.Y., and 32272544 to B.L.), Earmarked Fund for CARS (grant no. CARS-23 to Z.G.), Beijing Key Laboratory for Pest Control and Sustainable Cultivation of Vegetables (grant no. N/A to Y.Z.), and Science and Technology Innovation Program of the Chinese Academy of Agricultural Sciences (grant no. CAAS-ASTIP-IVFCAAS to Y.Z.). This research was also supported by European Research Council Advanced Grant (grant no. 788949 to T.C.J.T.). **Author contributions:** Conceptualization: Z.Y., Z.G., and Y.Z. Investigation: Z.Y., Z.G., C.G., J.X., Y.H., J.Z., X.Y., W.X., S.W., Q.W., and B.L. Methodology: Z.Y. and Z.G. Funding acquisition: Z.Y., Z.G., T.C.J.T., and Y.Z. Writing—original draft: Z.Y. and Z.G. Writing—review and editing: Z.Y., Z.G., W.Y., X.Z., T.C.J.T., and Y.Z. **Competing interests:** The authors declare that a patent has been filed to the China National Intellectual Property Administration (current status: substantive examination; applicant: Institute of Vegetables and Flowers, Chinese Academy of Agricultural Sciences; authors: Z.G., Z.Y., C.G., J.X., X.Y., W.X., S.W., Q.W. and Y.Z.; application date: 19 August 2022; application no. 202210995419.X). The authors declare no other competing interests. **Data and materials availability:** The full-length cDNA sequences of both cloned genes in this study have been deposited in the GenBank database (accession nos. ON513379 and ON513381). The metatranscriptome sequencing data in this study have been deposited in the SRA database (BioProject ID PRJNA874568). All data needed to evaluate the conclusions in the paper are present in the paper and/or the Supplementary Materials.

Submitted 18 April 2023
Accepted 3 January 2024
Published 2 February 2024
10.1126/sciadv.adi3105